INTEGRATED BIOMIMETIC SCAFFOLDS FOR SOFT TISSUE ENGINEERING

A THESIS SUBMITTED TO
THE GRADUATE SCHOOL OF NATURAL AND APPLIED SCIENCES
OF
MIDDLE EAST TECHNICAL UNIVERSITY

BY

SİNAN GÜVEN

IN PARTIAL FULFILLMENT OF THE REQUIREMENTS
FOR
THE DEGREE OF MASTER OF SCIENCE
IN
BIOTECHNOLOGY

JULY 2006

Approval of the Graduate School of Natural and Applied Sciences

Prof. Dr. Canan ÖZGEN
Director

I certify that this thesis satisfies all the requirements as a thesis for the degree of Master of Science

Prof. Dr. Fatih YILDIZ
Head of Department

This is to certify that we have read this thesis and that in our opinion it's fully adequate, in scope and quality, as a thesis for the degree of Master of Science in Biotechnology

Assoc. Prof. Dr. Kezban ULUBAYRAM
Co-supervisor

Prof. Dr. Nesrin HASIRCI
Supervisor

Examining Committee Members

Prof. Dr. Savaş KÜÇÜKYAVUZ (METU, CHEM) _____

Prof. Dr. Nesrin HASIRCI (METU, CHEM) _____

Prof. Dr. Sevda MÜFTÜOĞLU (Hacettepe Unv., HIST) _____

Assoc. Prof. Dr. Özdemir DOĞAN (METU, CHEM) _____

Prof. Dr. Suzan KINCAL (METU, CHE) _____

I hereby declare that all information in this document has been obtained and presented in accordance with academic rules and ethical conduct. I also declare that, as required by these rules and conduct, I have fully cited and referenced all material and results that are not original to this work.

Name, Last name: Sinan Güven

Signature:

ABSTRACT

INTEGRATED BIOMIMETIC SCAFFOLDS FOR SOFT TISSUE ENGINEERING

Güven, Sinan
M.S., Department of Biotechnology
Supervisor: Prof. Dr. Nesrin Hasırcı
Co-Supervisor: Assoc. Prof. Dr. Kezban Ulubayram

July 2006, 71 pages

Tissue engineering has the potential to create new tissue and organs from cultured cells for transplantation. Biodegradable and biocompatible scaffolds play a vital role in the transfer of the cultured cells to a new tissue. Various scaffolds for soft tissue engineering have been developed, however there is not any structure totally mimicking the natural extracellular matrix (ECM), ready to use.

In this study biodegradable and biocompatible scaffolds were developed from natural polymers by tissue engineering approach and tested *in vitro*. Scaffolds (SCAF) were prepared with freeze drying and composed of chitosan, gelatin and dermatan sulfate. Polymer solutions were treated with different stirring rates (500 rpm and 2000 rpm), freezing temperatures (-20 °C and -80 °C) and molding (cylindrical mold and petri dish) to achieve porous structure in order to provide sufficient space for cell growth and extracellular matrix production. Among the prepared scaffolds at different conditions, the

scaffolds prepared at 500 rpm and frozen at -80 °C, (SCAF-1), was chosen for further studies. These scaffolds achieved 0.512 MPa tensile strength, with 9.165 MPa tension modulus and 3.428 MPa compression modulus. Besides in lysozyme containing degradation medium they conserved their integrity and lost about 30 % of their initial weight in 30 days period. Mechanical and enzymatic degradation tests showed that scaffolds have physical integrity for the tissue engineering applications. To mimic the natural tissue and enhance cell growth, biologically active arginine – glycine - aspartic acid - serine (RGDS) peptides and platelet derived growth factor-BB (PDGF-BB) were immobilized on the SCAF-1. Fibroblast cells were seeded on the scaffolds containing RGDS, (SCAF-1-RGDS), and PDGF-BB, (SCAF-1-RGDS-PDGF), and incubated in media either free of serum or containing serum. Scaffolds immobilized with RGDS and PDGF-BB had the highest attached cell number by the day 15. Florescence microscopy studies also indicated that RGDS and RGDS-PDGF modified scaffolds were more suitable than controls, (SCAF-1), for cell growth and proliferation. According to scanning electron microscopy (SEM) results, modified scaffolds demonstrated better cell morphology and attachment of cells. Based on the obtained results, it can be concluded that RGDS-PDGF immobilized chitosan-gelatin-dermatan sulfate systems have a great potential to be used as a scaffold for soft tissue engineering applications.

Keywords: Tissue engineering, biomimetics, scaffold, chitosan, RGDS, growth factor.

ÖZ

YUMUŞAK DOKU MÜHENDİSLİĞİNE YÖNELİK BÜTÜNLEŞİK BİYOMİMETİK TAŞIYICI YAPILAR

Güven, Sinan
Yüksek Lisans, Biyoteknoloji Bölümü
Tez Yöneticisi: Prof. Dr. Nesrin Hasırcı
Ortak Tez Yöneticisi: Doç. Dr. Kezban Ulubayram

Temmuz 2006, 71 sayfa

Doku mühendisliği transplantasyon için kültür ortamında çoğaltılmış hücrelerden yeni doku ve organlar oluşturma potansiyeline sahiptir. Biyobozunur ve biyouyumlu taşıyıcı yapılar, kültür ortamında çoğaltılmış hücrelerin yeni dokuya aktarılmasında hayati bir role sahiptir. Bugüne kadar yumuşak doku mühendisliğine yönelik birçok taşıyıcı yapı geliştirilmesine karşın doğal ekstraselüler matrisi (ECM) tamamıyla taklit edebilen bir taşıyıcı yapı elde edilememiştir.

Bu çalışmada doku mühendisliği yöntemiyle doğal polimerlerden biyobozunur ve biyouyumlu taşıyıcı yapılar geliştirilmiş ve *in vitro* koşullarda test edilmiştir. Kitosan, jelatin ve dermatan sülfattan oluşan taşıyıcı yapılar dondurup-kurutma yöntemiyle üretilmiştir. Hücre büyümesi ve sentezlenen ECM için yeterli, gözenekli bir yapı elde edebilmek için polimer çözeltileri değişik karıştırma hızları (500 rpm ve 2000 rpm) ile hazırlamış, değişik kalıplar (silindirik ve petri kabı) kullanılmış ve iki farklı sıcaklıkta dondurulmuştur (-20 °C

ve -80 °C). Değişik koşullarda hazırlanmış olan yapılar arasından 500 rpm ile karıştırılanmış ve -80 °C'de dondurulmuş olanlar (SCAF-1) ileriki çalışmalarda kullanılmak üzere seçilmiştir. Bu taşıyıcı yapılar 0.512 MPa gerilme mukavemeti, 9.165 MPa gerilme modülüsü ve 3.428 MPa sıkıştırma modülüsüne sahip olup lizozom içeren ortamda 30 günde ağırlığının % 30'unu kaybetmekle birlikte fiziksel bütünlüğünü korumuştur. Mekanik ve enzimatik bozunma testleri geliştirilen yapının fiziksel anlamda doku mühendisliği uygulamalarına uygun olduğunu göstermiştir. Doğal dokuyu taklit edebilmek ve hücre büyümesini artırmak amacıyla biyolojik aktif arjinin-glisin-aspartik asit-serin (RGDS) peptitleri ve pleteletlerden elde edilen büyüme faktörü-BB (PDGF-BB) seçilen taşıyıcı yapıya immobilize edilmiştir. Yapılara fibroblast hücreler ekilip, RGDS ve PDGF-BB'nin etkisini görebilmek için inkübasyon serumsuz ve serumlu hücre kültürü ortamında gerçekleştirilmiştir. Hücre çoğalmaları, floresan mikroskobu ve taramalı elektron mikroskobu çalışmaları RGDS ve PDGF-BB bağlanan yapıların en yüksek hücre tutunması ve çoğalması ve doğru hücre morfolojisine sahip olduğunu göstermiştir. Elde edilen sonuçlara göre RGDS-PDGF immobilize edilmiş kitosan-jelatin-dermatan sülfat taşıyıcı yapıları yumuşak doku mühendisliği uygulamalarında kullanılabilme potansiyeline sahiptirler.

Anahtar Kelimeler: Doku mühendisliği, biyomimetik, taşıyıcı yapı, kitosan, RGDS, büyüme faktörü.

To My Dear Family,

ACKNOWLEDGEMENTS

I would like to express my appreciation to Prof. Dr. Nesrin Hasırcı and Assoc. Prof. Dr. Kezban Ulubayram for their valuable guidance and encouragement.

I would also like to express my appreciation to Prof. Dr. Sevda Müftüoğlu, Dr. Kemal Şerbetçi and Elif Vargün for their help and guidance.

I also wish to give my special thanks to all my friends. I am especially grateful to Esra Pınardağ, Yeliz Tunç, Tuğba Endoğan, Ersin Baykara, Aysel Kızıltay and Cantürk Özcan for their valuable help, friendship and moral support.

Especially, I am grateful to my parents, Sebile and Zülküf Güven and also to Emel Arıkan for their support, understanding, and love.

TABLE OF CONTENTS

LIST OF TABLES

LIST OF FIGURES

LIST OF ABBREVIATIONS

3D:	Three dimensional
3DP:	Three dimensional printing
BSA:	Bovine serum albumin
CAD:	Computer assisted design
CAM:	Computer assisted manufacturing
DMF:	N,N-dimethyl formide
DS:	Dermatan sulfate
ECM:	Extracellular matrix
EDC:	1-ethyl-3dimethylaminopropyl carbodiimide
EDTA:	Ethylenediamine tetraacetic acid
ELISA:	Enzyme-linked immunosorbent assay
EM:	Electron Microscopy
FCS:	Fetal calf serum
FDA:	United States Food and Drug Administration
FDM:	Fused deposition modeling
FTIR-ATR:	Fourier Transform Infrared Spectrometer-Attenuated Total Reflectance
GAG:	Glycosaminoglycan
GF:	Growth factor
KBr:	Potassium bromide
MTT:	3-(4, 5-dimethylthiazol-2-yl)-2, 5-diphenyltetrazolium bromide
NHS:	Hydroxysuccinimide
OD:	Optical density
PBS:	Phosphate buffer saline
PCL:	Poly(ε-caprolactone)
PDGF-BB:	Platelet derived growth factor – BB

PEG:	Poly(ethylene glycol)
PEO:	Poly(ethylene oxide)
PGA:	Poly(glycolic acid)
RGD:	Arginine-Glycine-Aspartic acid
RGDS:	Arginine-Glycine-Aspartic acid-Serine
RPMI:	Roswell Park Memorial Institute
PLA:	Poly(lactic acid)
PLGA:	Poly(lactide-*co*-glycolic acid)
PLLA:	Poly(L-lactide)
SDS:	Sodyum dodecyl sulfate
SEM:	Scanning electron microscope
SFF:	Solid freeform fabrication
SLS:	Selective laser sintering
UV:	Ultraviolet

CHAPTER 1

INTRODUCTION

"It was the best of times, it was the worst of times
It was the age of wisdom, it was the age of foolishness
It was the epoch of belief, it was the epoch of incredulity
We had everything before us, we had nothing before us"
Charles Dickens A Tale of Two Cities

1.1 Tissue Engineering

There are various traditional approaches to deal with the loss of tissue or non-functional tissues and these involve (a) surgical strategies that concern organ transplantation from one individual to another, tissue transfer from a healthy site to an affected site in the same individual, (b) replacement of tissue function with mechanical devices (such as prosthetic valves / joints and dialysis machines) (c) medical strategies include pharmacologic supplementation of the metabolic products of targeting tissue [1].

A new interdisciplinary field called tissue engineering raised during last two decades concerning on developing biomimetic cell-biodegradable carrier constructs for *in vivo* applications. First tissue engineering definition was made in 1988 at National Science Foundation meeting as:"… the application of the principles and methods of engineering and the life science toward the fundamental understanding of structure-function relationships in normal and pathological mammalian tissue and the development of biological substitutes to restore, maintain or improve functions" [2]. The innovative approach of tissue engineering is; to seed isolated cells

with tissue inducing substances, such as growth and differentiation factors [3], on a scaffold which mimics the extracellular matrix (ECM) and serves as a cell attachment, proliferating, migrating and functioning environment (Figure 1.1). After maturation in a bioreactor, cell seeded carrier can be implanted into the body and by time the carrier degrades while the cells proliferate, synthesize their native ECM, and take place of the natural tissue [4].

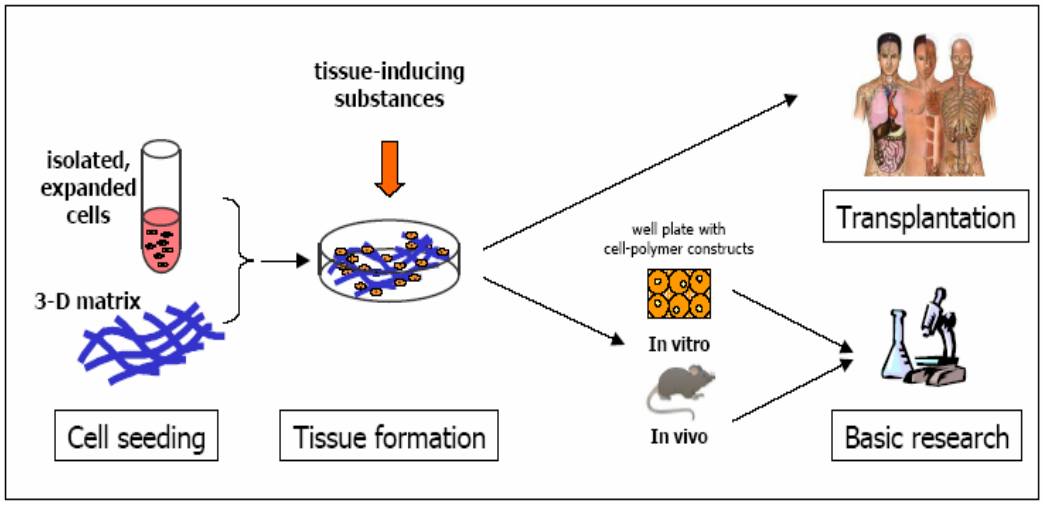

Figure 1.1 Diagram of tissue engineering approach [5].

1.2 Components of Tissue Engineering

1.2.1 The Cells

Cells used in tissue engineering could be drawn from primary tissues or cell lines. Primary tissues may be (i) xenogeneic, from different species, (ii) allogeneic, from different members of the same species, (iii) syngeneic, from a genetically identically individual, or (iv) autologous, from the same individual. Currently, the use of

xenogeneic and allogeneic cells in the engineered cell / polymer constructs is limited because of host immunosuppression. However, developments in cell science may enable to render cells immunologically safe so that clinical use of banked xenogeneic / allogeneic cells may become possible.

On the other hand, cell lines obtained from genetically modified cells can have the ability to proliferate forever. These cells have the potential for rapid proliferation *in vitro*, however several limitations such as the possible invocation of an immune response, the tendency for cell lines to lose differentiated function raise in this approach.

Most of the tissue engineering studies up to date using cell / polymer construct technology have employed primary autogenous cells and succeed to discard the drawbacks of previously mentioned approaches [1].

1.2.2 Scaffolds

Cell adhesion to ECM is essential to tissue homeostasis. In order to enable cell proliferation, migration and functionality, cells should be anchored on a substrate usually called scaffold [6, 7]. The officially accepted definition of a scaffold is; "The support, delivery vehicle, or matrix for facilitating the migration, binding, or transport of cells or bioactive molecules used to replace, repair, or regenerate tissues" [8].

1.2.2.1 Properties of Scaffolds

An ideal scaffold designed to engineer tissues must have several basic requirements, which include being; (i) three dimensional and highly porous with an interconnected pore network with a high surface area

to volume ratio for cell or tissue growth and flow transport of nutrients and metabolic waste; (ii) nontoxic, biodegradable or bioresorbable with a controllable degradation and resorption rate to match cell or tissue growth *in vitro* and/or *in vivo*; (iii) suitable surface chemistry for cell attachment, proliferation, and differentiation; (iv) mechanical properties to match those of the tissues at the site of implantation; and (v) be easily processed to form the desired shapes and sizes [9, 10].

1.2.2.2 Scaffolding Materials

Polymers (macromolecules) are the primary materials for scaffolds in various tissue engineering applications. Polymeric scaffolding materials can be broadly classified as either natural or synthetic.

1.2.2.2.1 Natural Biodegradable Polymers

Natural polymers, such as proteins and polysaccharides are widely used for tissue engineering applications. Collagen, gelatin, alginate, chitosan, chondroitin sulfate etc. can be considered in this class. Natural polymers provide advantage of possessing specific biological activities. Previous classical selection criterion for a safe material in biomedical implants dictated as choosing inert materials. However, in 1994, Peppas and Langer showed that such materials may cause cellular response [11]. While naturally occurring biomaterials are most closely simulate the native cellular environment, but large batch-to-batch variations upon isolation from biological tissues is the main limitation for their wide applications. Poor mechanical performances is also a drawback for transplantation scaffolds made from natural polymers, such as collagen and chitin, which cannot be easily melted with heat but require a special solvent [12, 13]. Decellularized tissues may also serve as natural materials for

scaffolding purposes. Removing cells from tissue usually require physical, enzymatic and chemical treatment where the major challenge is the elimination of all cellular materials and chemicals. In addition there are risks to degrade or lost the biological activity of the ECM. However there are decellularization protocols that have received regulatory approval for use in human patients, including human dermis (Alloderm®, LifeCell, Corp.), porcine urinary bladder (ACell, Inc.), and porcine heart valves (Synergraft®, CryoLife, Inc.) [14].

Collagen

The collagens are a family of fibrous proteins that occur in almost all mammalian tissues, constituting approximately 30 % of total protein mass in the mammalian body. They are particularly abundant in load bearing tissues such as tendon, bone and connective tissues. The primary feature of a typical collagen molecule is long, stiff, triple stranded helical structure (Figure 1.2), in which three collagen polypeptide chains, called α chains, are wraped around one another in a rope like superhelix. Because of relative ease of extraction and its abundance, collagens in their native and denatured forms had a long history of use as implantable materials. Its use has been facilitated by the fact that its amino acid sequences are highly conserved across different species boundaries. Thus, collagens from xenogenic sources like bovine and porcine generally produce only mild immune response. To date, 20 types of collagens have been identified. The form that has been most studied for scaffolding purposes in tissue engineering is Type I collagen, which is also the most abundant form (more than 90 % of all fibrous proteins) [15-18].

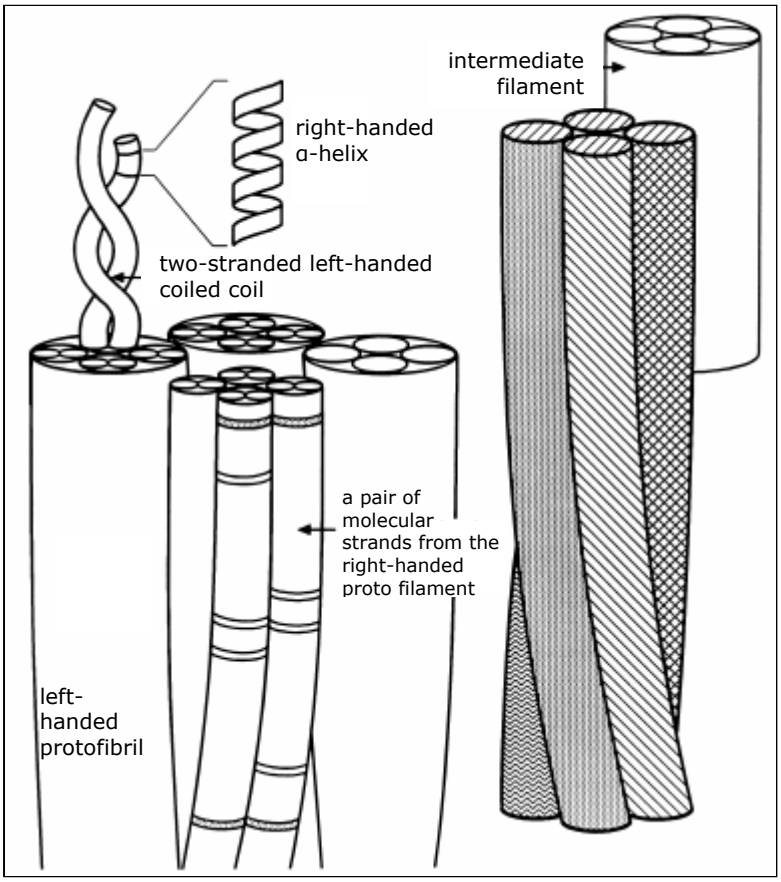

Figure 1.2 Schematic representation of collagen [19].

Gelatin

Gelatin is partially denatured derivative of the fibrous insoluble protein collagen, composed of a unique sequence of 19 amino acids and obtained by hydrolytic cleavage of collagen chains. Structurally, gelatin molecules contain repeating sequences of glycine (Gly)- A-B triplets, where A and B frequently are proline (Pro) and hydroxyproline (Hypro) (Figure 1.3). Gelatin is preferred to collagen since in some cases collagen expresses antigenicity in physiologic conditions while gelatin is not known to have any such antigenicity

[20]. Gelatin has been shown to exhibit activation of macrophages and high hemostatic effects. It is biocompatible, completely resorbable *in vivo*, and its physicochemical properties can be suitably modulated because of the existence of many functional groups. These characteristics have contributed to gelatin's proven record of safety as a plasma expander, as an ingredient in drug formulations, and as a sealant for vascular prostheses [21]. Gelatin can form a polyelectrolyte complex with chitosan at the suitable pH values [22].

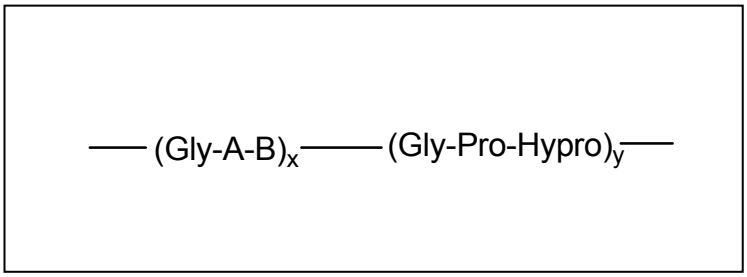

Figure 1.3 General structure of gelatin.

Two different types of gelatin can be produced depending on the method in which collagen is pretreated, prior to the extraction process [23]. The alkaline process targets the amide groups of asparagine and glutamine, and hydrolyses them into carboxyl groups, thus converting many of these residues to aspartate and glutamate. In contrast, acidic pretreatment does little affect on the amide groups present. As a result, pretreatment processes cause electrically different charged gelatin molecules. Alkaline pretreated gelatin is more cationic and has lower isoelectric point than acidic processed gelatin. Since that feature is adjustable it enables to get gelatin with various isoelectric point values [24].

Chitosan

Chitosan is derivative of chitin, the basic structural polymer in arthropod exoskeletons. Chitin is a high molecular weight glycopolymer composed of *N*-acetyl-D-glucosamine units linked via β(1→4) glycosidic bonds. Chitosan obtained by deacetylation of chitin is composed of (1→4)-2-amino-2-deoxy-β-D-glucose and (1→4)-2-acetoamido-2-deoxy-β-D-glucose units (Figure 1.4).

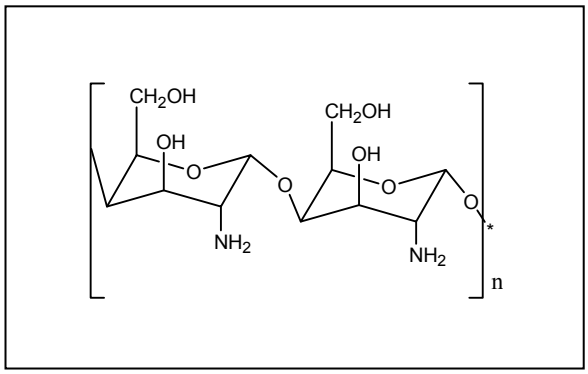

Figure 1.4 Structure of chitosan

Considering the chemical structure, chitosans are very similar to cellulose (Figure 1.4). Chitosan crystalline structure results in the polymer being insoluble in neutral or basic aqueous solutions. However, in dilute acids (pH < 6) free amino groups are protonated and crystalline structure is disrupted and dissolved. When the pH is raised, amino groups become deprotonated and form hydrogen bonding.

The repeated structure of chitosan contains glucosamine and N-acetylglucosamine which are found in glycosaminoglycans (GAGs).

GAGs play a major role in organizing and determining the properties and functionality of extracellular matrix (ECM). Being similar to GAGs structure makes chitosan a very preferable polymer in mimicking the natural tissue. However, free amino groups of chitosan make it cationic whereas GAGs are sulfated and have anionic nature. This feature may allow chitosan to interact with cellular receptors and matrix proteins in unique ways based on a combination of stereospecific glycan binding and nonspecific electrostatic interactions.

Compared to its analogue cellulose, chitosan can be hydrolyzed enzymatically in vivo. Lysozyme is major enzyme among pepsin, papain and pancreatin which appears to target acetylated residues [25]. The lysozyme-mediated degradation products are chitosan oligosaccharides of variable length. The degradation rate is inversely proportional to the degree of deacetylation. Highly deacetylated chitosans are more crystalline than others and for that reason enzymes could not penetrate into the microstructures to achieve degradation reactions.

Chitosan implant materials have been found to evoke minimal immunogenic reactions. During a healing process formation of normal granulation tissue, often with accelerated angiogenesis, appears to be the typical process [26-28]. In the short term (< 10 days), significant accumulation of neutrophils in the vicinity of the implants is often seen, but this dissipates rapidly and a chronic inflammatory response does not develop. Moreover, release of growth factors and cytokines by stimulated macrophages may induce local fibroblast and endothelial cell proliferation. In addition, this leads to formation of a highly cellular and well vascularized repair, followed by integration of the chitosan implant with the host tissue.

Another most important feature of chitosan is its ability to be processed under mild conditions into structures suitable for the production of tissue scaffolds. Porous chitosan structures can be easily produced by a phase separation method involving freezing and lyophilization of chitosan solutions in suitable molds [29]. During the freezing process, ice crystals nucleate from solution and grow along the lines of heat flux. Exclusion of the chitosan from the ice crystal phase and subsequent ice removal by lyophilization generates a porous material whose mean pore size can be controlled by varying the freezing conditions. Some control over pore orientation can also be obtained by manipulating the direction of thermal gradients during freezing.

The mechanical properties of chitosan scaffolds are mainly dependent on the pore sizes, pore orientations and degree of deacetylation. Tensile testing of hydrated samples shows that porous membranes have greatly reduced elastic moduli (0.1 – 0.5 MPa) compared with nonporous chitosan membranes (5 – 7 MPa). The elongation of porous membranes varied from values similar to nonporous chitosan (~30 %) to greater than 100 % as a function of both size and orientation of the pores [30, 31].

1.2.2.2.2 Synthetic Biodegradable Polymers

Poly(glycolic acid) (PGA), poly(lactic acid) (PLA), and their copolymers poly(lactic acid-co-glycolic acid) (PLGA) are a family of linear aliphatic polyesters, which are most frequently used in tissue engineering [32]. Relatively hydrophilic nature of PGA causes rapid degradation in aqueous solutions or *in vivo*, and loss of mechanical integrity in two - four weeks [33]. PLA is also widely used for scaffold fabrication. The extra methyl group in the PLA repeating unit (compared to PGA) makes it more hydrophobic, reduces the molecular affinity to water,

and leads to a slower hydrolysis rate. It takes many months or even years for a PLA scaffold or implant to loss mechanical integrity in vitro or *in vivo* [34]. To achieve intermediate degradation rates in between PGA and PLA, various lactic and glycolic acid ratios can be used to synthesize PLGAs. These polymers (PLA, PGA, and PLGAs) are among the few synthetic polymers approved by the US Food and Drug Administration (FDA) for certain human clinical applications.

There are other linear aliphatic polyesters, such as poly(ε-caprolactone) (PCL) [35], polyethylene glycol (PEG) also known as polyethylene oxide (PEO) [36]. PCL degrades at a significantly slower rate than PLA, PGA, and PLGA. The slow degradation makes PCL less attractive for general tissue engineering applications, but more attractive for long term implants and controlled release applications. PEG is petroleum derived synthetic water soluble polymer. It is nontoxic, nondegradable and is able to resist protein binding. Handling in mild conditions makes PEG and its derivatives to be preferred as versatile polymeric biomedical and tissue engineering materials.

1.2.2.3 Scaffold Preparation Techniques

Porous scaffolds can be fabricated using a variety of methods. These methods include woven or nonwoven preparation from spun fibers, blown films using solvents or propellants, or sintered polymer particles. Polymers are often supplied in solid pellet form which is often not suitable to fit tissue engineering demands. The choice of the correct preparation technique, however, is vital because the fabrication can significantly alter the properties of the material and its degradation characteristics.

1.2.2.3.1 Traditional Techniques

Fiber felts or meshes

Fiber meshes consist of individual fibers either woven or knitted into three-dimensional patterns of variable pore size. The advantageous characteristic features of fiber meshes are a large surface area for cell attachment and a rapid diffusion of nutrients in favor of cell survival and growth. However, they lacked the structural stability necessary for *in vivo* use [37].

Fiber bonding

Interconnected fiber networks have been prepared by Mikos et al., by the so-called fiber bonding technique [38]. Basically polymer fibers are aligned in the shape of the desired scaffold and then embedded in a solvent. After evaporation of the solvent, polymer is heated above the melting temperature. After all, polymer fibers are physically joined at their cross-points. Obviously, this technique is not most appropriate for the fine control of porosity. Choice of solvent and melting temperature restricts the general application of the technique to all polymers. Solvent remaining in the scaffold may cause undesired toxic effects to the cells and organs.

Phase separation

The polymer is dissolved in a solvent such as molten phenol, naphthalene or dioxane at a low temperature. Liquid-liquid or solid-liquid phase separation is induced by lowering the solution temperature. Subsequent removal of the solidified solvent-rich phase by sublimation leaves a porous polymer scaffold. One prominent advantage is to incorporate bioactive molecules into the matrices

without decreasing the activity of the molecule due to harsh chemical or thermal environments. A slight change in the parameters, such as types of polymer, polymer concentration, solvent/nonsolvent ratio, and the most importantly, thermal quenching strategy, significantly affect the resultant porous scaffold morphology [39].

Freeze Drying

Freeze drying is another scaffold preparation method which can give up to 90 % porosity. In this method dissolved and frozen polymer is lyophilized to form foam like porous scaffolds. Freezing temperature and heat flux during the freezing predict the scaffold mean pore size and orientation. Solvent crystallization takes part during the freezing and as the freezing rate is slower, pores form in larger sizes, since slow nucleation leads greater crystals which leave behind pores after the lyophilization. Heat flux determines the orientation of the crystals and therefore the pores [29].

Solvent casting and particulate leaching

This method consists of dispersing calibrated mineral (e.g., sodium chloride, tartrate and citrate) or organic (e.g., saccharose) particles in a polymer solution. This dispersion is then processed either by casting or by freeze-drying in order to evaporate the solvent. The salt particles are eventually leached out by selective dissolution to produce a porous polymer matrix. Highly porous scaffold with porosity up to 93% and median pore diameters up to 500 μm can be prepared using this technique. One disadvantage of this method is that it can only be used to produce thin wafers or membranes up to 3-mm thick. However, three-dimensional structures can be manufactured from polymer membranes by laminating them together to form a three-dimensional matrix of the desired shape at higher thickness [13, 40].

1.2.2.3.2 Rapid Prototyping Techniques

Traditional preparation techniques are lack of precise control of the three-dimensional pore architecture of the scaffolds. These drawbacks are trying to be eliminated by using computer-assisted design and manufacturing (CAD/CAM) techniques.

Rapid prototyping technique also known as Solid Free Form Fabrication (SFF) mainly consists of Fused Deposition Modeling (FDM), Selective Laser Sintering (SLS) and Three Dimensional Printing (3DP). In FDM, dissolved polymer is loaded to computer controlled machine that has printing nozzle. Nozzle deposits polymer droplets that solidify when released and build the structure layer by layer. SLS uses laser beams to sinter polymer powder in powder bed. The interaction of the laser beam with the powder raises the local surface temperature to the glass transition temperature of the powder. This is just below the melting temperature. It results in particle bonding—fusing the particles onto each other and to the previous layer to form a solid. In 3DP method, objects are created by a layered printing process with adhesive bonding, using powder as the base material. Each layer of powder is selectively joined where the part is to be formed by ink-jet printing of a binder material. The process is repeated layer by layer until the part is complete. However, the smallness of the powder particles and the binder drops are limited. The accuracy of positioning the printing nozzle is also limited. Besides rapid prototyping techniques have inherent shortcomings such as limited material selection and inadequate resolution. In addition, the resulting constructs have structural heterogeneity because of the drop assembly nature of the fabrication process. To overcome this shortcoming, a reverse fabrication technique has been developed to fabricate a negative replica of the scaffold. A polymer solution is cast into such a mold and solidified after the removal of the solvent. The

mold is then dissolved away to form the polymer scaffold with the designed three-dimensional pore network. The scaffold is more homogeneous and pore interconnectivity is developed but the feature resolution is improved [31, 41].

1.2.3 Cell Adhesive Peptides

Various polymers used in tissue engineering can be made attractive for cell interaction by modifying their surfaces so that recognition by cell membrane receptors is enhanced. These modifications are performed by coating ECM proteins such as fibronectin or immobilizing peptide molecules on the scaffolds. The Arginine-Glycine-Aspartic acid (RGD) sequence is by far the most effective and most often employed peptide sequence for stimulated cell adhesion on synthetic surfaces. This is based upon its widespread distribution and use throughout the organism, its ability to address more than one cell adhesion receptor, and its biological impact on cell anchoring, behavior and survival. In multicellular organisms contacts of cells with neighboring cells and the surrounding ECM are mediated by cell adhesion receptors. Among them the integrin family comprises the most numerous and versatile group. They play not only a major role as anchoring molecules but are also important in processes like embryogenesis, cell differentiation, immune response, wound healing and hemostasis [42].

In an attempt to reduce macromolecular ligands to small recognition sequences, RGDS was the first found peptide motif identified in 1984 by Pierschbacher and Rouslahti as a minimal essential cell adhesion peptide sequence in fibronectin (Figure 1.5) [43].

RGD peptides behave in two directions. They either inhibit cell adhesion to fibronectin or promote cell adhesion, when they are

immobilized on surfaces handoff the biomaterials. Since then, cell adhesive RGD sites were identified in many other ECM proteins, including vitronectin, fibrinogen, collagen, laminin, etc. [44].

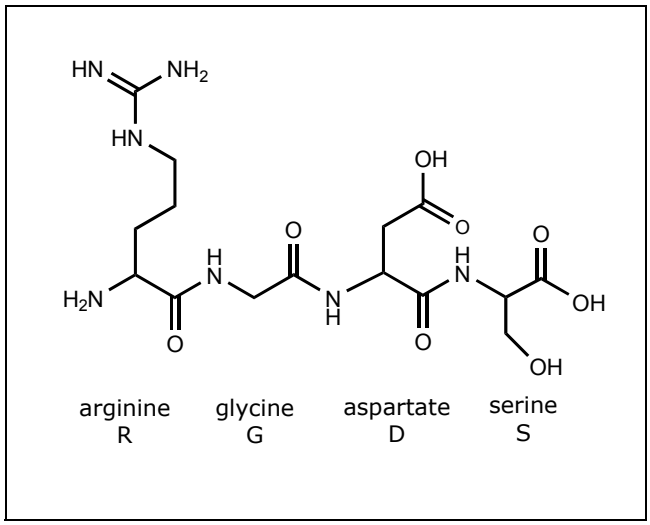

Figure 1.5 Chemical structure of Arg-Gly-Asp-Ser peptide.

1.2.4 Growth Factors

Growth factors are polypeptides that transmit signals to modulate cellular activities. Growth factors can either stimulate or inhibit cellular proliferation, differentiation, migration, adhesion and gene expression. There are several characteristic properties of growth factors. Many cell types can produce the same growth factor and the same growth factor can act on many cell types with the same or different effects. Growth factor effects are concentration-dependent, often in a complex non-monotonic way. Growth factors can influence the secretion and action of other growth factors.

Growth factors usually exist as inactive or partially active precursors that require proteolytic activation, and may need to bind to matrix

molecules for activity or stabilization. Growth factors have short biological half-lives. Platelet derived growth factor (PDGF) has two chains each containing 124 and 109 amino acids (Figure 1.6), isolated from platelets, can not be detected in the circulation and has a half life of less than 2 minutes when injected intravenously [45, 46].

Platelet-derived growth factor-BB has been demonstrated to stimulate the proliferation and recruitment of both fibroblast cells in vitro [47]. Due to its capability in promoting wound healing through enhancing the formation of granulation tissues, recombinant human PDGF-BB has been approved by US Food and Drug Administration (FDA) for use in diabetic foot ulcers [48].

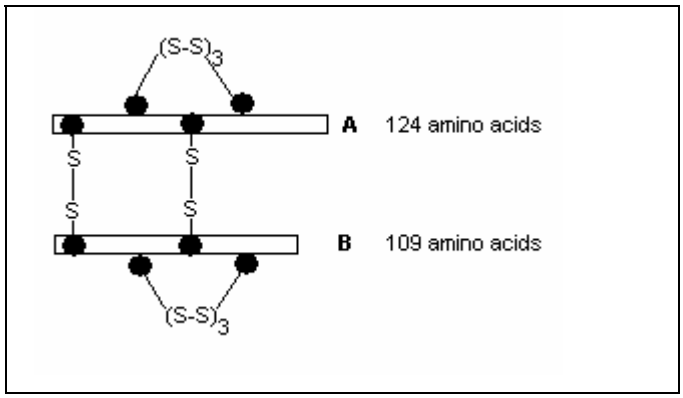

Figure 1.6 General representation of Platelet Derived Growth Factor-BB

1.3 Natural Extracellular Matrix Organization

Two main classes of extracellular macromolecules form up the matrix; (1) polysaccharide chains of the class called glycosaminoglycans (GAGs), which are usually found covalently linked to protein in the form of proteoglycans, and (2) fibrous proteins, including collagen,

elastin, fibronectin, and laminin, which have both structural and adhesive functions.

The proteoglycan molecules in connective tissue form a highly hydrated, gel-like ground substance in which the fibrous proteins are embedded. The polysaccharide gel resists compressive forces on matrix while permitting the rapid diffusion of nutrients, metabolites, and hormones between blood and the tissue cells. The collagen fibers both strengthen and help to organize the matrix and rubberlike elastin fibers give resilience.

Glycosaminoglycans

Glycosaminoglycans are unbranched polysaccharide chains composed of disaccharide units where one of the two sugars is always an amino sugar which in most cases is sulfated. GAGs are highly negatively charged and hydrophilic. They constitute less than 10 % of the weight of fibrous proteins. But because they form porous hydrated gels, the GAG chains fill most of the extracellular space, providing mechanical support to the tissue. Four main groups of GAGs are distinguished according to their sugars and type of linkage between sugars, and the number and location of sulfate groups: (1) hyaluronan, (2) chondroitin and dermatan sulfate, (3) heparin sulfate, and (4) keratin sulfate. Chemical structure of Dermatan sulfate is given in Figure 1.7.

Fibrous Proteins

Although collagen fibers give the ECM great tensile strength, their rigid, rodlike structure is not particularly suited to the elasticity and flexibility required by some tissues. For example, lung tissue must expand and contract as an organism breathes, and arteries must be able to dilate and constrict as the heart pumps blood through them.

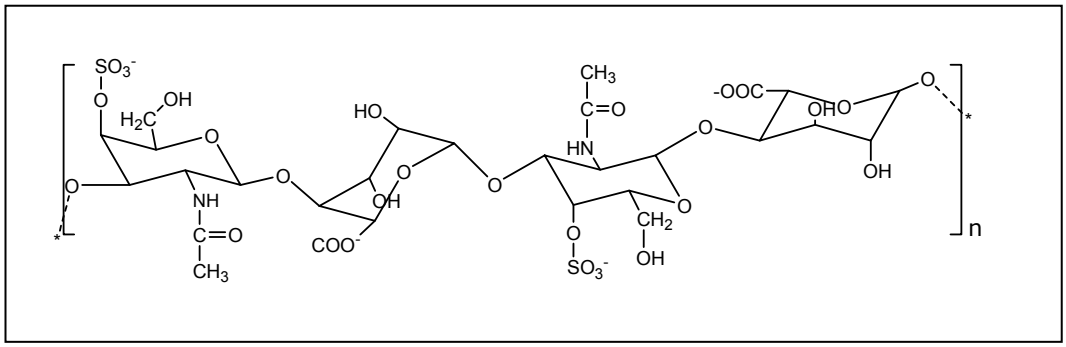

Figure 1.7 Chemical structure of Dermatan sulfate.

Other tissues that require a flexible ECM include skin and the intestines, which change shape continuously. Elasticity is provided by stretchable elastic fibers present in the ECM. The principle constituent of elastic fibers is a family of ECM proteins called elastins. Like collagens, elastins are rich in amino acids of glycine and proline. However, the proline residues are not hydroxylated and no hydroxylysine is present. Elastin molecules are crosslinked to one another by covalent bonds between lysine residues. Tension on an elastin network causes the individual molecules to adopt extended conformations that permit the overall network to stretch. When the tension is released, the individual molecules relax, returning to their normal, less extended conformations. The crosslinks between molecules then cause the network to recoil to its original shape [49].

Proteins in the natural extracellular space are either of the structural type (for example, collagen, elastin) or the adhesive type (for example, laminin, fibronectin).

Collagen is the most abundant protein found in the ECM and is secreted by chondrocytes, fibroblasts, and other cell types. Several chemically distinct forms of collagen have been identified, each of which contains the same basic macromolecular unit: an alpha helical

chain formed by the interaction of three polypeptides (Figure 1.2). These polypeptide chains contain 1000 amino acids in length and have a certain sequence specific to each type of collagen. The most common forms of collagen found within the ECM are types I, II, III, and IV. Following secretion into the ECM, molecules of collagen types I, II, and III organize into larger fibrils which are 10 to 300 nm in diameter. These fibrils are stabilized by crosslinks which connect lysine residues within or between adjacent collagen molecules. In some tissues these fibrils become further organized, forming larger collagen fiber several micrometers in diameter. Fibrillar collagens interact with cells trough integrin receptors on cell surfaces. Cell differentiation and migration during development are influenced by fibrillar collagens. In contrast to the fibrillar collagens, collagen type IV forms a mesh-like lattice that constitutes a major part of the mature basal lamina, the thin mat separating epithelial sheets from other tissues. Collagen type IV interacts with cells indirectly by binding to laminin, another major component of the basal lamina.

Fibronectin is a dimeric glycoprotein composed of similar subunits, each containing 2500 amino acids. The two similar polypeptide chains are linked by disulfide bonds at the carboxyl termini and folded into a number of globular domains. The biological activities of certain polypeptide domains within the fibronectin macromolecule have been defined by observing the properties of fibronectin fragments. Fibronectin binds to collagen and heparin; this binding contributes to the organization of the ECM. Integrin receptors on cell surfaces bind to a fibronectin domain containing the tripeptide sequence of RGD. It appears that complete cellular adhesion also requires participation of another region on fibronectin, the "synergy" region on the amino terminus side of the RGD containing region. Cellular interactions with fibronectin have been shown to affect cell morphology, migration, and differentiation.

Laminin is a large cross-shaped protein composed of three polypeptide subunits: α, β, and γ. At least twelve different heterotrimeric laminins are found in mammals. These different isomers has important role in neutrite growth, cell migration, and cell adhesion. Laminin contains binding sites for cell attachment and other binding sites that promote neutrite outgrowth. Regions that promote cell attachment, heparin binding, and neutrite outgrowth have been identified and involve the specific peptide sequences like RGD.

Elastin is a hydrophobic, nonglycosylated protein composed of 830 amino acids. After secretion into the ECM, extended elastin molecules form crosslinked fibers and sheets which can stretch and relax upon deformation. Elastin is found in abundance in tissues that undergo repeated stretching, such as the blood vessels.

Tenacin, a multiunit glycoprotein of $1.9x10^6$ daltons, has both cell adhesive and anti adhesive properties. While it is confined primarily to the nervous system in adults, it is present in embriyonic tissues and may be involved in modulating cell migration during embriyogenesis. Tenacin is composed of six polypeptide chains, some containing the RGD sequence, which are disulfide – linked to produce a windmill – shaped complex [50].

1.4 Aim of the Study

In this study an integrated biocompatible and biodegradable scaffolds which mimic the natural tissue extracellular matrix were developed by tissue engineering approach. Scaffolds were composed of chitosan, gelatin and dermatan sulfate and prepared under various stirring rates, freezing temperatures and moldings to achieve sufficient pore size and organization for cell growth and proliferation. Biologically active arginine-glycine-aspartate-serine (RGDS) peptide and platelet derived growth factor (PDGF) were immobilized on to the scaffolds to enhance adhesion and proliferation of seeded fibroblast cells. Designed scaffolds were tested *in vitro* in order to show their potent to be used in soft tissue engineering area.

CHAPTER 2

MATERIALS AND METHODS

2.1 Materials

Chitosan (medium molecular weight), gelatin (Type-A from porcine skin), dermatan sulfate β-heparin, Arg-Gly-Asp-Ser (RGDS) peptide, 1-ethyl-3dimethylaminopropyl carbodiimide (EDC), lysozyme (chicken egg white), hydroxysuccinimide (NHS), platelet derived growth factor BB-human (PDGF-BB), RPMI (Roswell Park Memorial Institute) basal cell culture medium, 3-(4, 5-dimethylthiazol-2-yl)-2, 5-diphenyl tetrazolium bromide (MTT), sodium dodecyl sulfate (SDS), propidium iodide, and osmium tetroxide were purchased from Sigma–Aldrich, Germany. N,N-dimethyl formide (DMF), acetic acid, absolute ethanol, sodium hydroxide were supplied from Reidel-de-Haën, Germany. Gluteraldehyde solution was purchased from Fluka, Switzerland. Phosphate buffer saline (Dulbecco, 1x, PBS) was purchased from Biochrom AG, Germany. BIOAMF® basal medium was supplied from Biological Industries Ltd., Haemek, Israel. Glycerol, sodium cacodylate and gluteraldeyde (electron microscopy grade) were purchased from BDH Chemicals, England.

2.2 Methods

2.2.1 Preparation of Chitosan/Gelatin/Dermatan Sulfate Scaffolds

Chitosan (2 % w/v) was dissolved in 0.2 M acetic acid at room temperature and stirred 24 h to obtain homogeneous solution. On the other hand gelatin (2 % w/v) was dissolved in 0.2 M acetic acid at

40 °C and dermatan sulfate (DS) solution (0.6 % w/v in deionized water) was added drop wise to gelatin solution till the final concentration will be 0.03 g DS / 2 g gelatin and stirred for 30 min. Homogenized chitosan solution was mixed with gelatin-dermatan sulfate solution in 4:1 (v/v) ratio and stirred for 1 h with magnetic stirrer at 500 rpm. Final solution was composed of 79.7 % chitosan, 20 % gelatin and 0.3 % dermatan sulfate. This homogeneous solution poured into polypropylene cylindrical molds (14 mm in diameter, 60 mm in height) or polystyrene petri dishes (35 mm in diameter, 7 mm in height), frozen at -80 °C for 12 h and lyophilized for 48 h (Christ® Alpha 1.4 Germany). These scaffolds were coded as SCAF-1. All scaffold preparations were performed under room temperature conditions.

To examine the effects of stirring rate and freezing temperature on scaffold morphology and structure, the given procedure was performed at two different stirring rates; 500 rpm (1 h) and 2000 rpm (15 min) with magnetic stirrer and overhead mixer, respectively and frozen at two different temperatures (-20 °C and -80 °C). The obtained four set of scaffolds are given in Table 2.1.

Table 2.1 Prepared scaffolds

Scaffold	Stirring Rate	Freezing Temperature
SCAF-1	500 rpm	-80 °C
SCAF-2	500 rpm	-20 °C
SCAF-3	2000 rpm	-80 °C
SCAF-4	2000 rpm	-20 °C

2.2.2 Stabilization of Scaffolds and Peptide Immobilization

Scaffold stabilization and immobilization of RGDS peptides were achieved in one step process. Freeze dried scaffolds were immersed in absolute ethanol for 15 min, then immersed in peptide solution (composed of 25:25:1 v/v/v of the following solutions; 0.2 mM peptide in DMF, 2.5 mg/mL EDC in DMF and 8 mM NHS in pH 8.4 phosphate buffer) and kept at 4 °C for 72 h or 96 h to assure crosslinking and peptide immobilization [51]. Afterwards the scaffolds were washed with ethanol (40 %, 100 mL) twice and frozen at -80 °C overnight and then lyophilized for 24 h. These scaffolds were coded as SCAF-RGDS.

2.2.3 Incorporation of Growth Factor into the Scaffolds

Platelet Derived Growth Factor-BB (PDGF-BB 10 µg) was dissolved in sterile HCl solution (1 mL, 4 mM containing 0.1 % BSA). Required amounts of PDGF-BB solutions (200 ng/cm^3 scaffold)were added by an injector on disc shaped SCAF-1-RGDS scaffolds which have the size of 12 mm diameter and 2 mm height. Scaffolds were frozen overnight at -80 °C and then freeze dried. These scaffolds were coded as SCAF-1-RGDS-PDGF.

2.2.4 Characterization of Scaffolds

2.2.4.1 SEM Analysis

Scaffolds were coated with gold and their topography and porosity were analyzed via Scanning Electron Microscopy (SEM) (JEOL®, JSM-6400, NORAN Instruments, Tokyo, Japan).

2.2.4.2 FTIR-ATR Spectroscopy

Fourier Transform Infrared Spectrometer-Attenuated Total Reflectance (FTIR-ATR) spectra for the unmodified (SCAF), and RGDS-modified (SCAF-RGDS) scaffolds were obtained with a BRUKER® Vertex 70, (BRUKER®, Ettlingen, Germany) spectrophotometer. Spectra were analyzed with built-in OPUS Viewer 5.5® software. To assure the RGDS structure, FTIR spectrum of RGDS peptide was obtained in KBr pellet (Figure B.1 appendix).

2.2.4.3 Mechanical Tests

Mechanical stabilities of the prepared scaffolds were analyzed with LLOYD® LRX5K (LLOYD® Instruments Limited, Fareham, Hampshire, UK) mechanical tester. Dry scaffolds with 12 mm in diameter and 12 mm in height were compressed with 10 kg load capacity with a rate of 0.1 mm/min at room temperature.

2.2.4.4 Degradation Studies of Scaffolds

The biodegradation studies of the scaffolds were carried out *in vitro* by incubating the scaffolds in PBS (pH 7.4) containing $1x10^4$ U/mL of the enzyme, lysozyme, in an incubation dish and kept at 37 °C. At predetermined time intervals, the scaffolds were taken from the medium, washed with distilled water and freeze-dried and weighted. Weights remaining, W_r, were determined from the given formula,

$$\% W_r = (W_t / W_0) \times 100$$

where W_0 denotes the original weight, and W_t is the weight at time t [52]. Each biodegradation experiment was repeated three times and the average values were taken.

2.2.5 In-vitro Cell Culture Studies

The prepared scaffolds (SCAF-1, SCAF-1-RGDS, SCAF-1-RGDS-PDGF) (12 mm in diameter and 2 mm in height) were exposed to UV for 1 h prior to cell culture studies to achieve sterilization. Unmodified scaffold (SCAF-1) was used as a control for cell culture studies.

2.2.5.1 Cell Culture

Isolated human fibroblast cells were cultured in tissue culture plates (Falcon®) using BIOAMF® basal medium containing 10 % fetal calf serum (FCS), 2 mM L-glutamine and 1 % penicillin - streptomycin. Incubations were carried out at 37 °C in air containing 5 % CO_2 atmosphere and medium was changed every 3 days. At confluence fibroblasts were harvested by tripsinization. For this purpose, 5 mL tripsin-EDTA (0.05 % trypsin, 0.02 % EDTA) solution was added and the cultures were incubated at 37 °C for 15 min, centrifuged at 1200 rpm for 5 min resuspended and subcultured in the same medium. Cells used in seeding were 3rd passage.

2.2.5.2 Seeding of Scaffolds

Fibroblast cells in culture medium were seeded on scaffolds ($4x10^3$ cells/ 0.068 cm^3 scaffold) in 96-well tissue culture plate. Briefly, scaffolds initially were treated with RPMI basal cell culture medium for 30 min in two ways either in the cell culture medium containing FCS and L-glutamine or without FCS and L-glutamine. Harvested passage 3 cells were suspended with basal medium to inhibit the effect of trypsin, centrifuged at 1200 rpm for 5 min and the precipitated cell pellets were resuspended with basal medium either contains FCS and L-glutamine or not. 1 mL of cell containing medium was colored with trypan blue (1 mL, 10 %) and cells were counted by

applying through capillary to Thoma® cell count lam. $4x10^3$ cells were seeded on scaffolds (0.068 cm^3) present in 96 well tissue culture plate and incubated at 37 °C, in air containing 5 % CO_2 atmosphere and medium was changed in every 3 days.

2.2.5.3 Cell Proliferation Assay

MTT, (3-[4,5-dimethylthiazol-2-yl]-2,5-diphenyl tetrazolium bromide), assay was performed to observe viable cells on the scaffolds. For this purpose, seeded scaffolds in 96 well tissue culture plate were taken out in predetermined time intervals and placed in a new 96 well tissue culture plate and washed 3 times with PBS (pH 7.4). Then 10 µL MTT and 100 µL PBS were added to each well and the plate was incubated for 4 hours (37 °C, air 5 % CO_2). Then 100 µL, 10 % SDS solution was added on each scaffold and incubated overnight. Finally scaffolds were removed from wells and optical densities (OD) of aliquoids were measured with ELISA reader (TECAN SPECTRA® CLASSIC, Austria) at 492 nm [53]. Six independent OD values were obtained for each scaffold group and the average values were taken.

2.2.5.4 Preparation of Calibration Curve for MTT Assay

To quantify the cell number on the scaffolds; a calibration curve was prepared as follows: known amounts of fibroblast cells ($4x10^3$, $8x10^3$, $1.2x10^4$, $1.6x10^4$, $2x10^4$ cells) were seeded on 96 well tissue culture plate and after 2 hours of incubation at 37 °C in air containing 5 % CO_2, MTT assay was performed. Calibration curve was prepared by plotting the cell number versus OD obtained at 492 nm (Figure C.1 appendix).

2.2.5.5 Preparation of Fibroblast Seeded Scaffolds to SEM

Fibroblast seeded scaffolds both prepared in serum free and serum containing cell culture media were fixed for SEM observation. Briefly, scaffolds were washed with cacodylate buffer (0.1 M, pH 7.4) and treated with 2.5 % glutaraldehyde in cacodylate buffer (0.1 M, pH 7.4) for 2 hours at room temperature. Then scaffolds were washed with cacodylate buffer 3 times each 5 min and placed in 1 % osmium tetroxide solution (5 mL/scaffold) for 1 h at room temperature in dark. Next, scaffolds were washed again with cacodylate buffer (10 mL) 3 times for 5 min. Dehydration of scaffolds was carried out with ethanol in sequential steps (10 min in 25 %, 10 min in 50 %, 10 min in 75 %, 10 min in 85 %, 10 min in 95 %, and three times 10 min in 100 %) and vacuum dried [54]. Scaffolds were coated with gold, the attached cells and morphology of the cells were analyzed via Scanning Electron Microscopy (SEM) (JEOL®, JSM-6400, NORAN Instruments, Tokyo, Japan).

2.2.5.6 Preparation of Fibroblast Seeded Scaffolds to Florescence Microscopy

Fibroblast seeded scaffolds were frozen at -196 °C in liquid nitrogen. Sections with 7 µm thickness of frozen scaffolds were taken by cryostat (Leica® Jung Frigocut 2800E). Nuclei of fibroblast cells exist in the scaffolds were stained with propidium iodide (100 µL, 1 %) and examined under florescence microscope (Leica® DMR DC500) with build in software (IM 50®).

CHAPTER 3

RESULTS AND DISCUSSION

3.1 Preliminary Work in Scaffold Preparation

Various sets of chitosan, gelatin-dermatan sulfate polymer solutions were prepared with different concentrations and compositions in order to justify the proper preparation technique and scaffold composition.

Initially to examine the chitosan nature, scaffolds were prepared only from 1 % (w/v) chitosan in 0.1 M acetic acid polymer solution, stirred with 2000 rpm overhead mixer and freeze dried (Figure A.1). Observations and SEM images showed that chitosan is promising material in physical manner for scaffolding. Next, 1 % (w/v) chitosan and 1% (w/v) gelatin dissolved in 0.1 M acetic acid were mixed in 2.6:1 ratio respectively. Glycerol (2% v/v) was added to chitosan-gelatin solution as a plasticizer to obtain soft elastic scaffold and freeze dried (Figure A.2). The structure was elastic however removing the excess glycerol from scaffolds was difficult and required additional steps in process which flawed the scaffold structure. Therefore glycerol concentration was reduced to 1 % (v/v) while keeping the rest of the composition constant (Figure A.3). Then chitosan amount was increased and chitosan-gelatin ratio was set to 4:1, respectively (Figure A.4). Since the removal of excess glycerol was still problem, for further studies glycerol was removed from the scaffold composition. Addition of dermatan sulfate to chitosan-gelatin mixture was also studied (Figure A.5). Crosslinked scaffolds were prepared by using glutaraldehyde (Figure A.6). But for further studies, glutaraldehyde was not preferred, instead EDC/NHS was used since crosslinking and RGDS peptide immobilization on scaffols could be

achieved properly in one step with EDC/NHS. For non-crosslinked scaffolds preparation, effect of stirring rate was reduced from 2000 rpm to 500 rpm and well oriented pores were obtained (Figure A.7). These type of pore structures were not reported in literature previously. Therefore, it was decided to study the reproducibility and to increase physical strength via increasing chitosan and gelatin concentration from 1 % (w/v) to 1.5 % (w/v) in 0.1 M acetic acid. It was observed that increasing the polymer concentration did not alter the oriented pore structure but increased the physical strength (Figure A.8).

Scaffold preparation technique and scaffold composition that will be used in the study was developed with the results of the above mentioned preliminary work. Finally, the concentrations of each, chitosan and gelatin were set to 2 % (w/v) in 0.1 M acetic acid. For these scaffolds, the effects of two stirring rates (500 rpm and 2000 rpm), and two freezing temperatures (-20 °C and -80 °C) were examined.

3.2 Characterization of Biomimetic Scaffolds

Scaffolds used in tissue engineering applications should have high void volumes in order to allow cells migrate into and populate the scaffold to facilitate new tissue formation, vascularization and structural integration with the surrounding tissue [55]. Besides pore size, orientation is also critically important in determining the mechanical properties of the scaffold [56]. Porosity is defined as the percentage of void space in a scaffold and it is a morphological property independent of the scaffolding material [57]. However porosity of a scaffold can be controlled with the preparation technique and parameters. Therefore porosity and structural organization should

be optimized for the designed scaffolds before any tissue engineering usage.

3.2.1 Stirring Rate of Natural Polymers

Scaffold preparation solutions containing chitosan, gelatin and dermatan sulfate were stirred at two different rates, either at 500 rpm with a magnetic stirrer or at 2000 rpm with an overhead mixer. These scaffolds were molded either in polypropylene cylindrical molds (14 mm in diameter, 60 mm in height) or in polystyrene petri dishes (35 mm in diameter, 7 mm in height). Resulting SEM image (Figure 3.1a and c) of 3-D scaffold (SCAF-3) prepared with 2000 rpm shows well organized layered structure, however due to the high speed of stirring; bubble shaped polymeric structures filling the distances between the layers can be observed in the matrix. On the other hand, scaffolds prepared at 500 rpm (SCAF-1) demonstrated layered structures but in this case layer intervals were clear of bubbles (Figure 3.1b and d).

The major challenge in *in vitro* cell culture studies is dealing with the nutrient and waste material transport within the inner parts of the scaffolds prepared for tissue engineering applications. Cells on the upper side of scaffolds are more viable compared to cells inside the scaffold. Open pores and sheet like inner structure of scaffolds prepared at 500 rpm makes these scaffolds good candidates for efficient nutrient and waste circulation leading to successful cell attachment and proliferation. Therefore SCAF-1 and SCAF-2, prepared at 500 rpm, are thought to have potential to be used for cell culture studies.

3.2.2 Scaffold Molding and Freezing Temperature

The shape of molds in which polymer solutions are placed, is another critical issue on organizing the structure of the scaffolds. Scaffolds prepared in petri dishes at -80 °C, show nonuniform orientation and distribution of pores as shown in Figure 3.2a and c. Upper part of these scaffolds which were exposed to atmospheric conditions during freezing, show more bubble like polymeric formations in a dense structure with closed pores compared to inner part. Petri dishes are in 7 mm height and have large surface area (9.61 cm^2) and therefore it is assumed that freezing flux did not affect the polymer solution homogenously. Therefore the surface and bulk demonstrated different formations and the homogeneous inner parts which are also the appropriate parts for tissue engineering are very limited. For these reasons it is assumed that these scaffolds will not provide uniform cell seeding distribution and are not suitable for cell culture experiments.

In cylindrical molds with small inner diameter (14 mm) the freezing flux is assumed to be equally distributed though the whole polymer solution. That feature leads to creation of symmetrical ice nucleation when the samples were frozen and therefore after the freeze-drying well oriented sheet like laminar interconnected pores were obtained (Figure 3.2b).

Freeze drying technique gives porous scaffolds as a result of sublimation of solvent crystals formed with freezing. Freezing temperature affects the pore size and the pore shape of the scaffolds. Lower freezing temperatures induce crystal formation more rapidly [58]. Therefore solvent crystals formed in this way at lower temperatures are smaller than the crystals formed at higher temperatures.

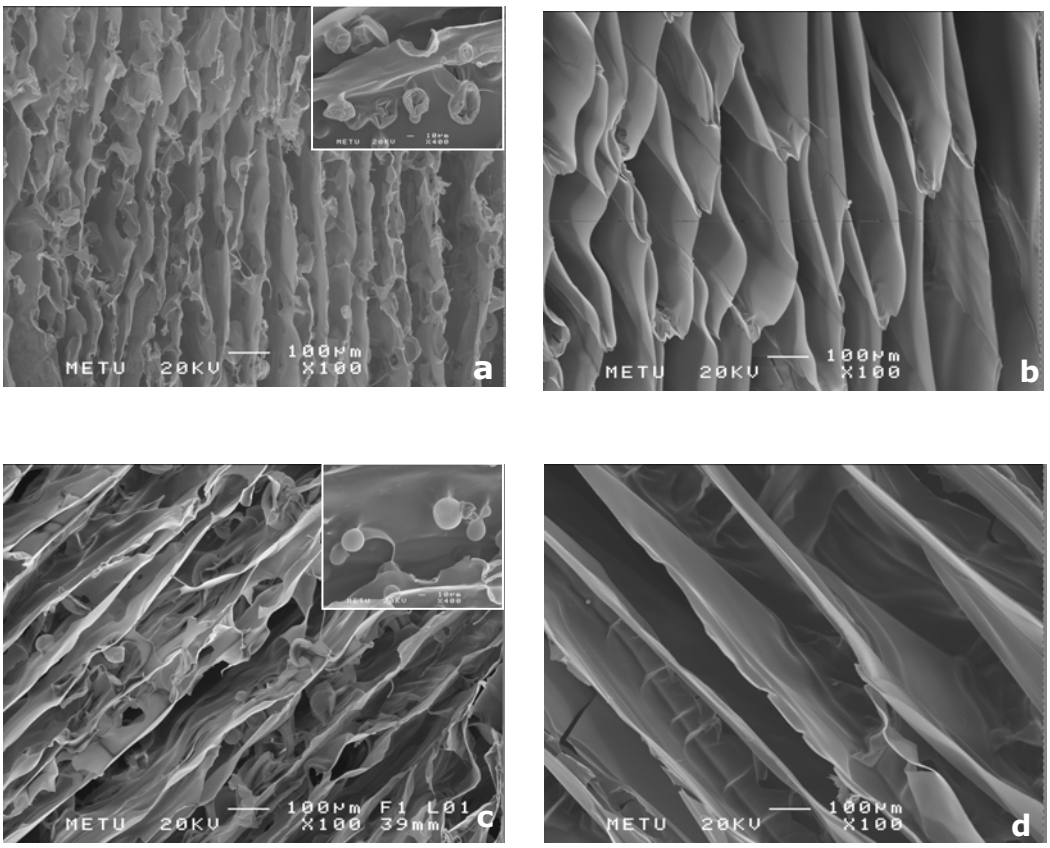

Figure 3.1 Effect of stirring rate of polymer solution on scaffold morphology. (a) SCAF-3 in petri dish (middle section), (b) SCAF-1 in petri dish (middle section), (c) SCAF-3 in cylindrical mold, (d) SCAF-1 in cylindrical mold.

In order to see the effects of freezing temperature on pore size between scaffold layers, polymer solutions prepared with in cylindrical molds with 500 rpm stirring rate were frozen at two different temperatures of -20 °C and at -80 °C. SEM micrographs are given in Figure 3.3. Average pore size between scaffold layers in -20 °C frozen scaffolds is about 200-400 μm (Figure 3.3a), whereas is about 100-150 μm in scaffolds frozen at -80 °C (Figure 3.3b). Having small pore size between layers in the scaffolds also indicate that there are more layers in unit volume of scaffold prepared at -80 °C. In fact this also implies that there will be more cell sheets per unit volume of scaffold.

Moreover, an increase in the void volume results in a reduction in mechanical strength of the scaffold [57]. Larger pores of SCAF-2 are suspected to lead greater void volumes and weaken the structure. For these reasons it was decided to use scaffolds (SCAF-1) prepared at -80 °C in cylindrical mold for cell culture experiments.

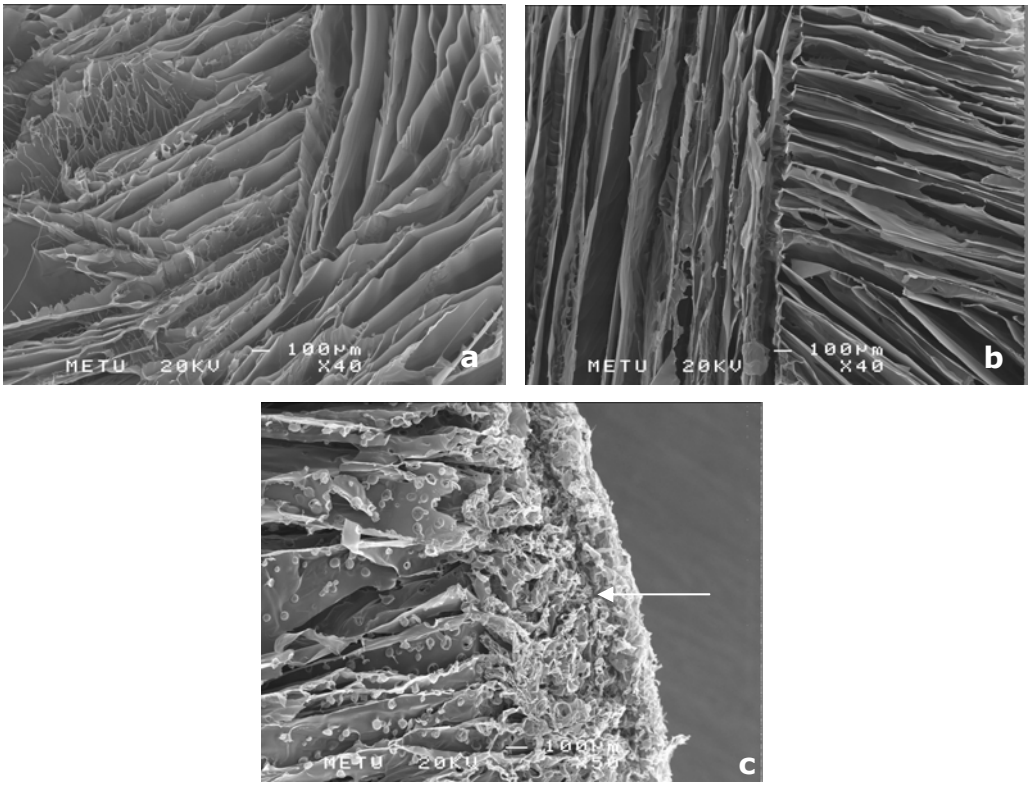

Figure 3.2 Molding effect on scaffolds (a) SCAF-1 in petri (middle section) (b) SCAF-1 in cylinder (middle part) (c) SCAF-3 in petri dish (arrow indicates upper section).

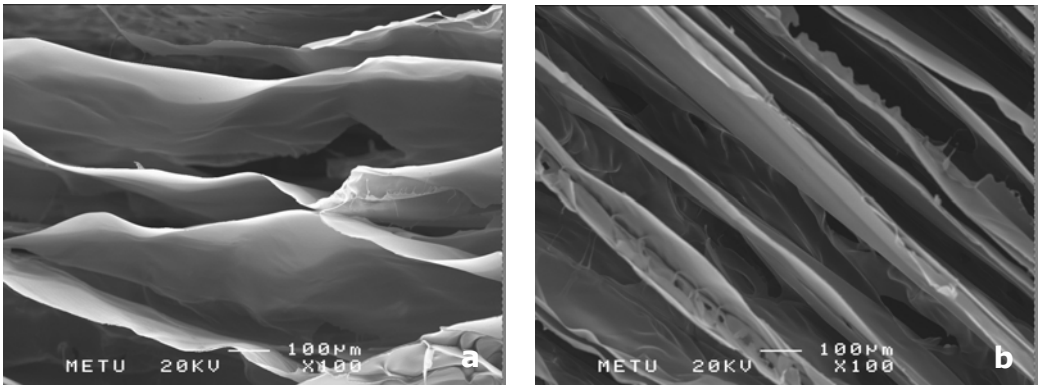

Figure 3.3 Effect of freezing temperature on the scaffolds, (a) SCAF-2, -20 °C (b) SCAF-1, -80 °C.

3.2.3 Mechanical Tests

Mechanical strengths of scaffolds prepared at 500 rpm and 2000 rpm stirring rate shaped in cylindrical molds, and frozen at -80 °C, were examined with a mechanical test instrument both in compression and tension manner in order to study the compression modulus, tension modulus and tension strength in dry conditions. Mechanical tests of the scaffolds in cylindrical mold were performed both before and after the crosslinking of scaffolds (SCAF-1 and SCAF-3) with EDC/NHS.

Compression tests were performed with cylindrical scaffolds 12 mm in diameter and 12 mm height. Compression modulus was obtained from the initial slope of load versus deformation graph. Compression resistance of non-crosslinked and crosslinked scaffolds (SCAF-1 and SCAF-3) was determined from compression modulus data. It could clearly be interpreted that crosslinking significantly increase the compression modulus values from 0.601 MPa to 3.428 MPa for SCAF-1 and from 0.741 MPa to 3.386 MPa for SCAF-3 (Table 3.1 and Figure 3.4). However there is no significant difference in compression modulus values between scaffolds prepared at 500 rpm (SCAF-1) and 2000 rpm (SCAF-3).

For tension tests, the specimens were prepared as follows; cylindrical scaffolds were uniformly compressed and thick sheets were obtained. These samples (SCAF-1 and SCAF-3) were properly placed to the holders of the mechanical tester. At those stages, ultimate attention was paid not to break the scaffolds. At tension tests all scaffolds broke off from the center part of the gage length. This is desired in all type of mechanical tests and indicates that the pressure applied during the preparation of sheets was uniformly applied. Tensile strength and tension modulus were calculated from the load versus deformation graphs and the results are given Table 3.1 and Figure 3.5 and 3.6. Crosslinking improves also the tension modulus and tensile strength of scaffolds. The tension modulus values for SCAF-1 (non-crosslinked) and SCAF-1 (crosslinked) were 7.333 MPa and 9.165 MPa, respectively while tensile strength values were O.300 MPa and 0.512 MPa. The tension modulus values were obtained as 9.106 MPa for SCAF-3 (non-crosslinked) and 9.408 MPa for SCAF-3 (crosslinked). Corresponding tensile strength values for SCAF-3 (non-crosslinked) and SCAF-3 (crosslinked) were found to be 0.456 MPa and 0.581 MPa, respectively.

Non-crosslinked and crosslinked scaffolds prepared at 2000 rpm (SCAF-3) have higher tension modulus and tensile strengths values than ones prepared at 500 rpm (SCAF-1) both before and after crosslinking (Figure 3.5-3.6). A probable explanation could be such that SCAF-3 has bubble like polymeric structures and therefore their void volumes are lower than the SCAF-1.

As a result, mechanical properties of SCAF-3 (crosslinking) were found to be slightly better than SCAF-1 (crosslinking). Hovewer as it mentioned before SCAF-1 with higher pore size yields efficient nutrient and metabolic waste transfer. Therefore SCAF-1, prepared with 500 rpm stirring rate, frozen at -80 °C in cylindrical molds and

crosslinked with EDC/NHS was chosen to be suitable for the following cell culture experiments.

Table 3.1 Mechanical test values of scaffolds

Scaffold	Compression Modulus (MPa)	Tension Modulus (MPa)	Tensile Strength (MPa)
SCAF-1 non-crosslinked	0.601±0.125	7.333±0.264	0.300±0.047
SCAF-3 non-crosslinked	0.741±0.020	9.106±2.045	0.456±0.025
SCAF-1 crosslinked	3.428±0.179	9.165±1.348	0.512±0.164
SCAF-3 crosslinked	3.386±0.052	9.408±1.367	0.581±0.157

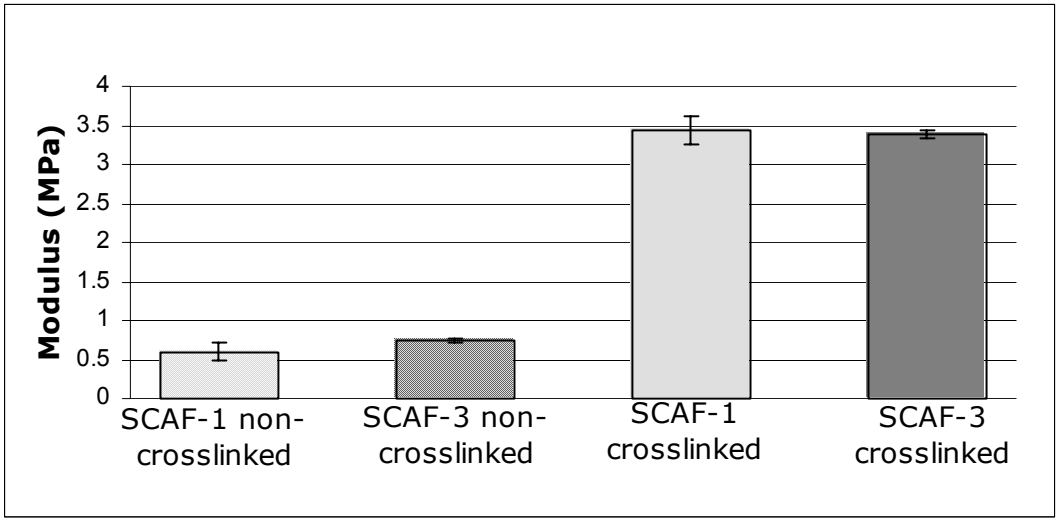

Figure 3.4 Compression modulus of crosslinked and non-crosslinked scaffolds (n>3).

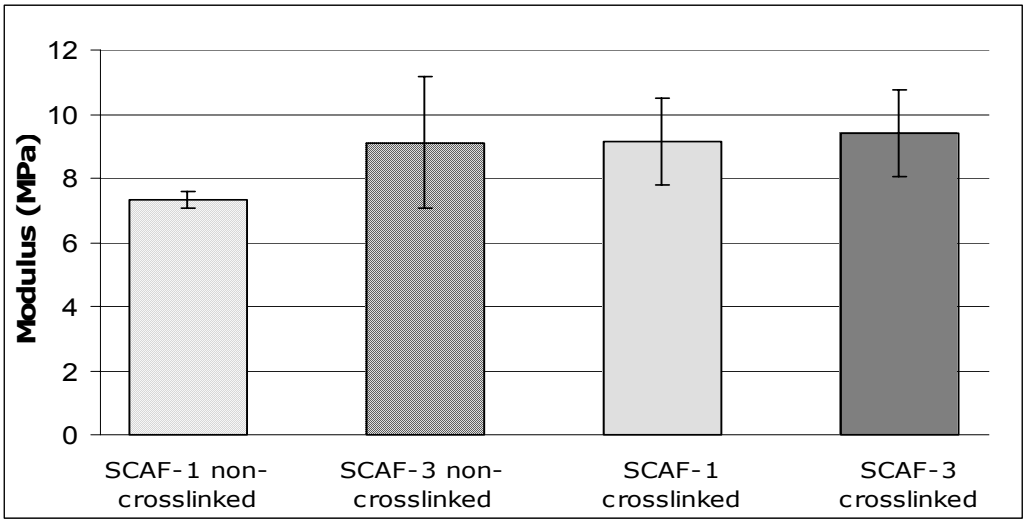

Figure 3.5 Tension modulus of crosslinked and non-crosslinked scaffolds (n>3).

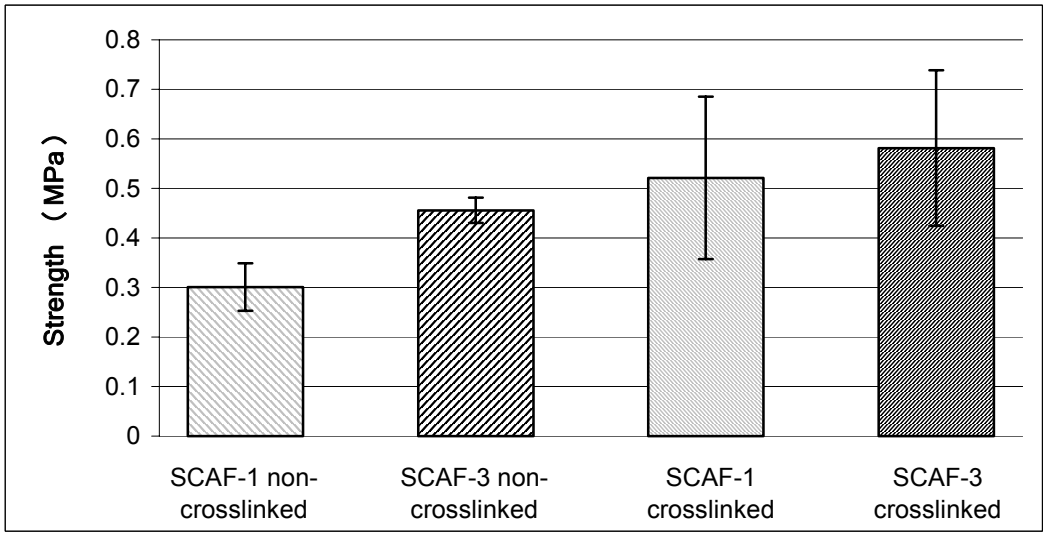

Figure 3.6 Tensile strength of crosslinked and non-crosslinked scaffolds (n>3).

3.2.4 Degradation Studies

Degradation kinetics is extremely important for a scaffold that is going to be used in tissue engineering applications. Scaffold should protect its structural properties inside the physiological, cell culture media and even *in vivo* after the implantation. Cell proliferation and functionalization takes time and therefore if scaffold degrades rapidly, cells will go apoptosis before the natural tissue formation since their carrier integrity is lost. On the other hand if the scaffold is very rigid and degradation time is too long there will be space restrictions at the implant site. In this study degradation experiments for crosslinked and non-crosslinked SCAF-1 scaffolds were performed *in vitro* at 37 °C in lysozyme containing PBS solution at pH 7.4. Lysozyme is a nonspecific proteolytic enzyme widespread in human and can hydrolyze chitosan [59]. Crosslinking efficiency of the scaffolds is one of the major parameters that control the degradation rate. Non-crosslinked scaffolds lost their integrity totally even after 2 h of incubation whereas crosslinked scaffolds conserved their integrity and lost about 30 % of their initial weight in 30 days period (Figure 3.7). In literature it is given that 25 days integrity is enough for skin wound healing process [60]. The degradation results of crosslinked scaffolds in this study excessively meet this condition and therefore it could be concluded that the crosslinking procedure used in this study is efficient for stabilizing the prepared scaffolds.

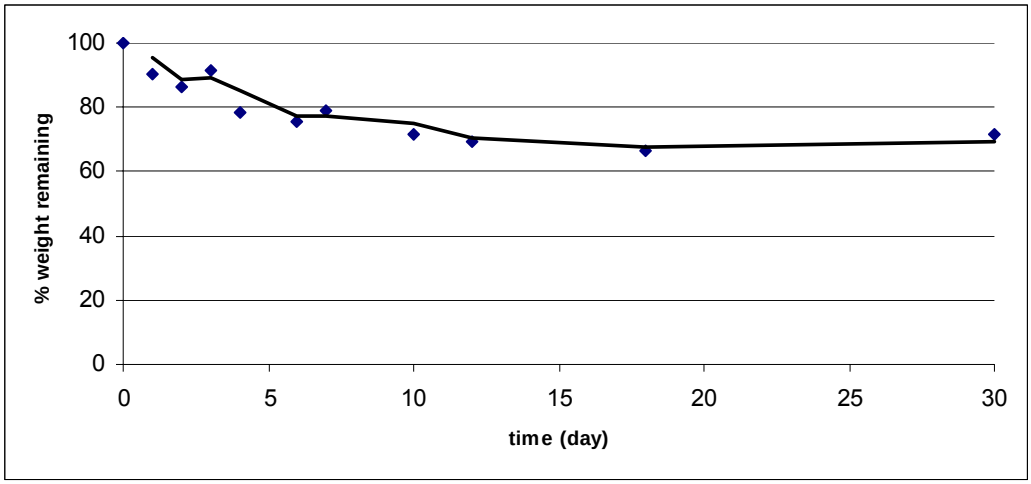

Figure 3.7 Degradation curve of SCAF-1 in lysozyme containing PBS pH 7.4 (n=3).

3.3 RGDS Immobilization

To enhance the cell adhesion through the integrin cell receptors and scaffolds, cell receptor recognizing sites were created on scaffolds by immobilizing Arg-Gly-Asp-Ser (RGDS) peptide. RGD sequences are present in fibronectin protein and serve as specific ligands for integrin receptors where fibronectin is responsible for cell adhesion. In this study immobilization of RGD on scaffolds was carried out in the presence of EDC and NHS which function as activators, form intermediates that lead formation of imide bonds between amino groups of chitosan and carboxylic acid groups of peptides. Water is nucleophilic, and hydrolysis can be a competing reaction during activation and coupling, especially at higher pH (>9–10). To reduce hydrolysis, surfaces are commonly activated in nonaqueous solvents [61]. Therefore the reaction was carried out in buffered basic (pH 8.4) organic media (DMF).

FTIR-ATR spectra of the non-modified scaffolds, (SCAF-1 and SCAF-3), and RGDS immobilized scaffolds (SCAF-1-RGDS and

SCAF-3-RGDS) were obtained (Figure 3.8 – 3.9). From the obtained spectra any significant differences that indicate the immobilization of RGDS peptide were not observed. Since the immobilization takes place through the amino groups of chitosan it was expected that after the coupling reaction, N-H bending peak should reduce or disappear. The reason for not being able to observe this reduction can be the presence of gelatin in the scaffold structure that may shield the disappearance of N-H bending peak at 1548 cm^{-1}. Gelatin is a partially denatured derivative of collagen protein and it also contains amino acids which may mask the difference among the RGDS peptide immobilized and non-immobilized spectra. To confirm that idea, the scaffolds that does not contain gelatin (SCAF-Ch) were prepared and coupled with RGDS peptide with the same concentrations and procedure. The FTIR-ATR spectra of non modified scaffold that does not contain gelatin (Figure 3.10c) and the one which is RGDS immobilized (Figure 3.10b) show a clear reduction of N-H bending peak at 1548 cm^{-1} which confirms the successful immobilization of RGDS to the scaffolds. Extending the immobilization time from 72 h to 96 h makes the coupling much effective where the indicator peak almost disappeared (Figure 3.10a).

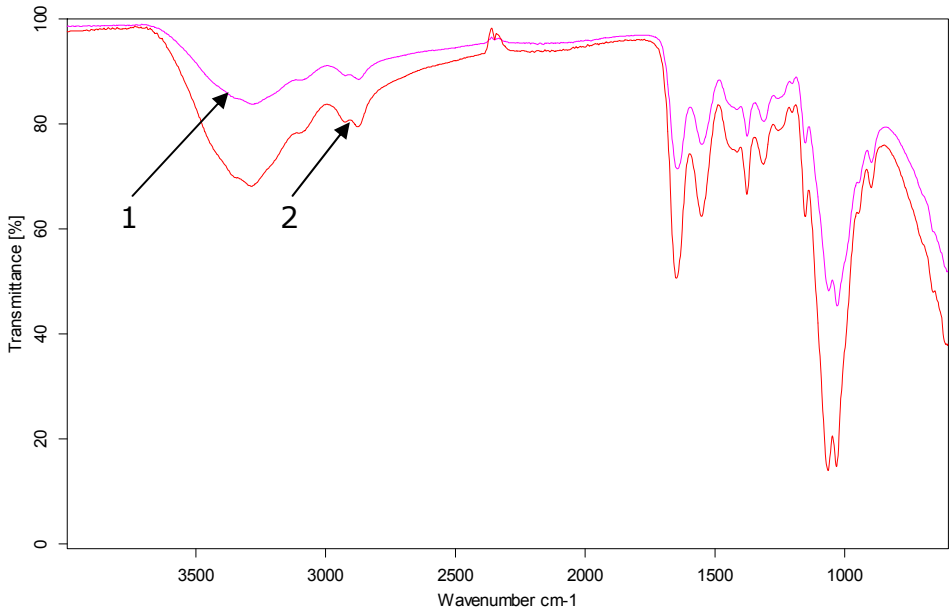

Figure 3.8 FTIR-ATR spectra of scaffolds (1) SCAF-1, (2) SCAF-1-RGDS.

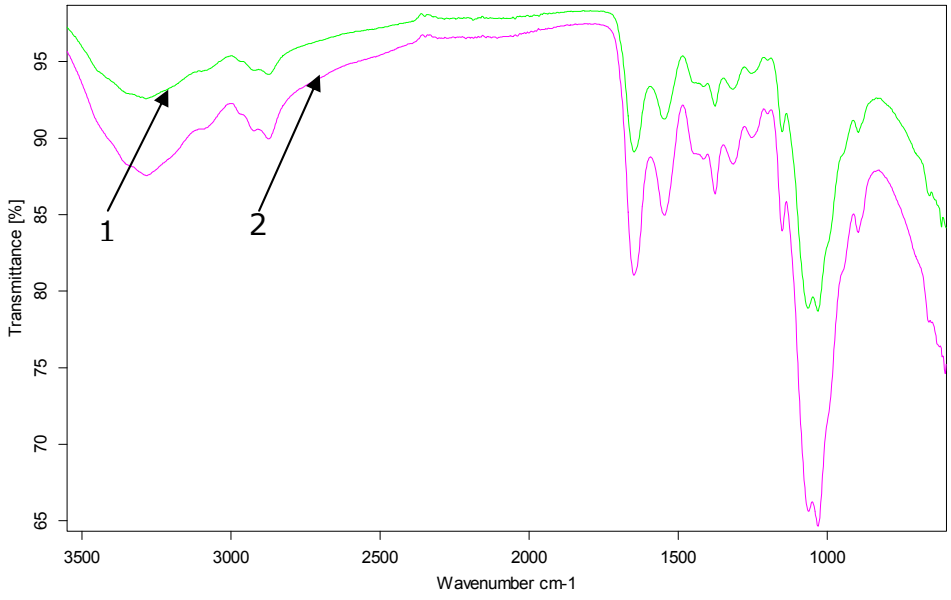

Figure 3.9 FTIR-ATR spectra of scaffolds (1) SCAF-3, (2) SCAF-3-RGDS.

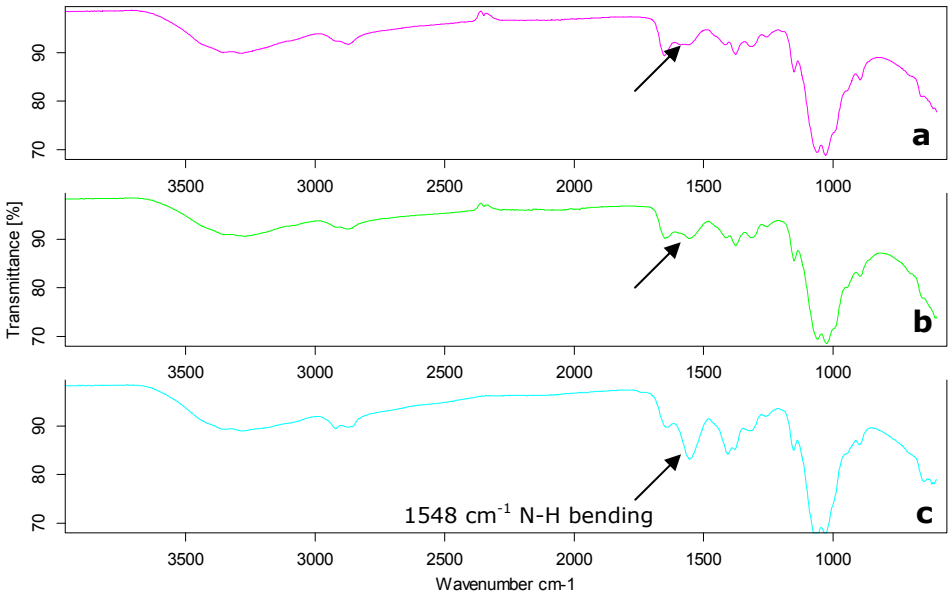

Figure 3.10 FTIR-ATR spectra of (a) SCAF-Ch-RGDS (96 h), (b) SCAF-Ch-RGDS (72 h), (c) SCAF-Ch.

3.4 Optimized Scaffolds

The parameters, (stirring rate of natural polymer solution, freezing temperature and molding shape) that may affect the scaffold morphology are used as variables in order to produce a scaffold suitable for tissue engineering applications. According to the obtained results, optimum scaffold is chosen as the one which prepared in cylindrical mold with 500 rpm stirring rate, frozen at -80 °C, immobilized with RGDS and crosslinked with EDC/NHS (SCAF-1-RGDS) (Figure 3.11). For cell culture experiments these scaffolds were selected and used after the incorporation of PDGF-BB.

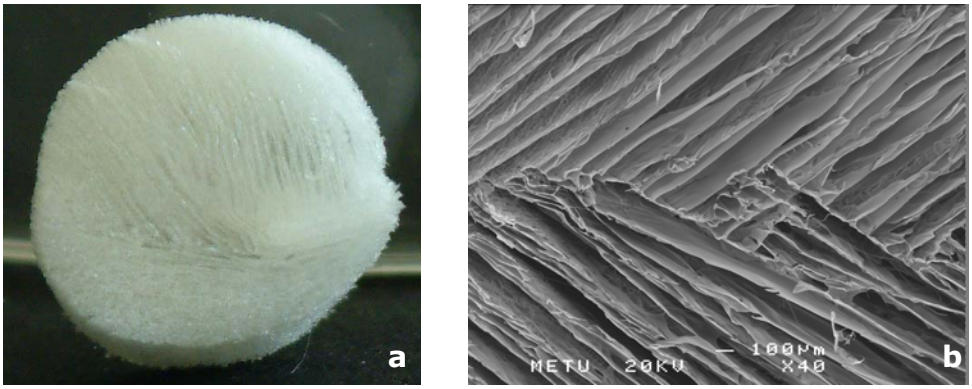

Figure 3.11 Optimized 3-D scaffolds (a) Photograph, (b) SEM image

3.5 Growth Factor Incorporation

Platelet derived growth factor–BB was incorporated to RGDS immobilized scaffolds. PDGF-BB (10 μg/mL) was dissolved in BSA (0.1 %) containing dilute HCl (1mL, 4 mM) and put on the scaffolds in the concentration of 200 ng/cm^3 scaffolds. PDGF-BB is anionic molecule and since the scaffolds are chitosan based they are cationic, therefore there is an electrostatic interaction between PDGF-BB and scaffold. That feature makes the PDGF-BB stay on the scaffolds, not to burst to the cell culture medium causing an inactivation or denaturation.

3.6 Cell Culture Studies

Cell culture studies were performed both in serum containing and serum free culture media.

3.6.1 Serum Free Proliferation

Integrin binding ligand RGDS and PDGF-BB immobilized SCAF-1 scaffolds (SCAF-1-RGDS and SCAF-1-RGDS-PDGF respectively) were

selected for cell culture studies. Nonmodified SCAF-1 was used as control. Cells were amplified in fetal calf serum containing cell culture medium, however since some growth factors are present in fetal calf serum and may mask the effect of PDGF immobilized on the scaffolds, one set of proliferation studies were performed in serum free cell culture medium.

Viability and proliferation of cells were determined by MTT assay at predetermined time intervals. Calibration curve was prepared to calculate the viable cell numbers from optical density values (Figure B.2 appendix). Live cells uptake the yellow MTT tetrazolium salt, cleave it and form purple formazan crystals. Number of live cells can be obtained through the optical densities measured by ELISA reader with 492 nm filter by using the calibration curve [62]. This procedure was applied and on day 5, cell numbers and proliferation percentages for control and SCAF-1-RGDS were found to be quite low as ~1600 cells and ~4 % respectively (Table 3.2 – 3.3), (Figure 3.12 – 3.13). On the other hand presence of PDGF-BB increased cell number to 2350 and proliferation to 15.5 %. On day 15 the proliferation percentage values for all scaffolds were above 90 %. PDGF-BB immobilized scaffolds are more active for cell proliferation (150.8 %) than other scaffolds as it is expected.

Table 3.2 Cell numbers on scaffolds obtained from MTT assay at 492 nm in serum free media on day 2, day 5 and day 15

	Cell Number		
Scaffold	**Day 2**	**Day 5**	**Day 15**
SCAF-1 (control)	1579	1643	3033
SCAF-1-RGDS	1762	1820	3763
SCAF-1-RGDS-PDGF	2033	2350	5100

Table 3.3 Percent proliferation of cells on scaffolds in serum free media on day 5 and day 15

	% Proliferation	
Scaffold	**Day 5**	**Day 15**
SCAF-1 (control)	4.1	92.1
SCAF-1-RGDS	3.3	113.5
SCAF-1-RGDS-PDGF	15.6	150.8

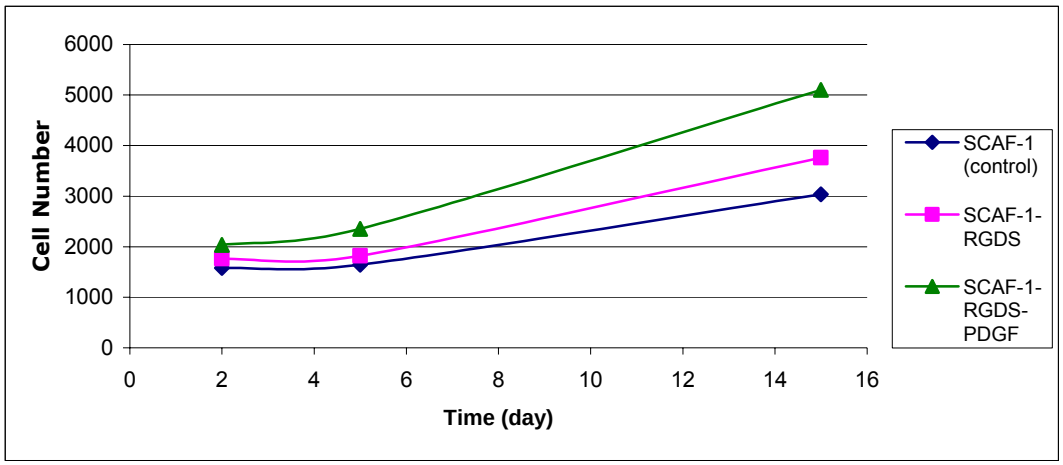

Figure 3.12 Proliferation curves of fibroblast cells on scaffolds in serum free medium, SCAF-1 (control), SCAF-1-RGDS and SCAF-1-RGDS-PDGF (OD at 492 nm), (n=6).

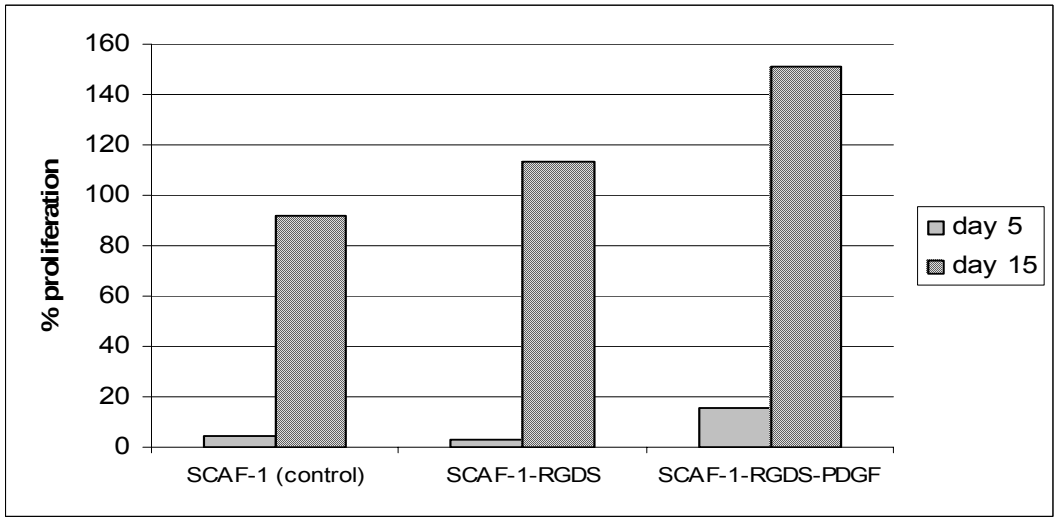

Figure 3.13 Percent proliferation of fibroblasts seeded on scaffolds in serum free medium between day 5 and day 10, (OD at 492 nm), (n=6).

3.6.2 Serum Containing Proliferation

The same set of scaffolds from section 3.6.1 were incubated in FCS containing cell culture medium to evaluate the activity of the prepared biomimetic scaffolds in the presence of serum. The cell proliferation curve and percentage proliferation values for scaffolds are found to be highest for RGDS-PDGF immobilized ones, similar to the ones cultivated in serum free media (Table 3.4 – 3.5), (Figure 3.14 – 3.15). These data interpret that serum in cell culture media masks the activity of PDGF immobilized on scaffolds.

Table 3.4 Cell numbers on scaffolds obtained from MTT assay at 492 nm in serum containing media on day 2, day 5 and day 15

	Cell Number		
Scaffold	**Day 2**	**Day 5**	**Day 15**
SCAF-1 (control)	2435	2300	5358
SCAF-1-RGDS	2050	2380	5745
SCAF-1-RGDS-PDGF	2240	2367	6275

Table 3.5 Percent proliferation of cells on scaffolds in serum containing media on day 5 and day 15

	% Proliferation	
Scaffold	**Day 5**	**Day 15**
SCAF-1 (control)	-5,5	120.1
SCAF-1-RGDS	16.1	180.2
SCAF-1-RGDS-PDGF	5.7	180.1

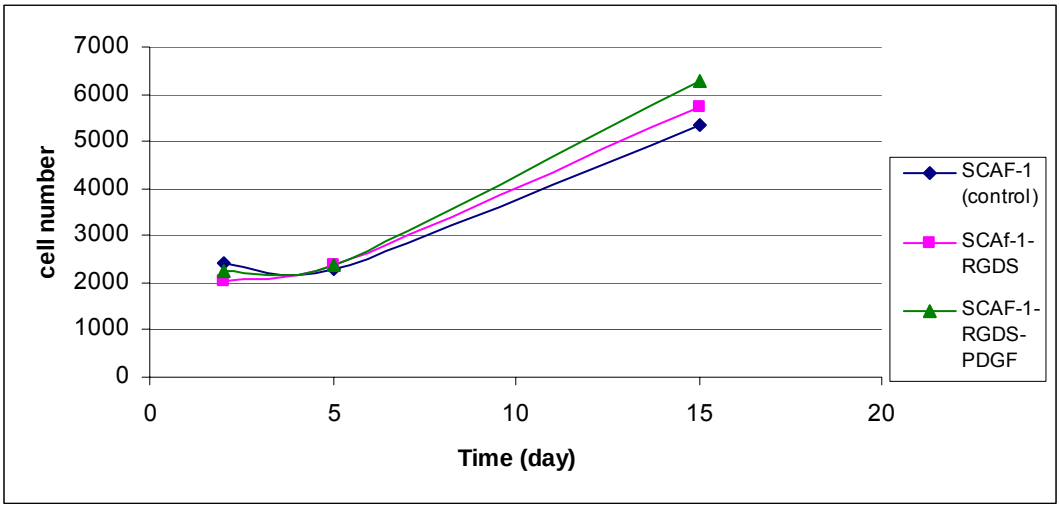

Figure 3.14 Proliferation curves of fibroblast cells on scaffolds in serum containing medium, SCAF-1 (control), SCAF-1-RGDS and SCAF-1-RGDS-PDGF (OD at 492 nm), (n=6).

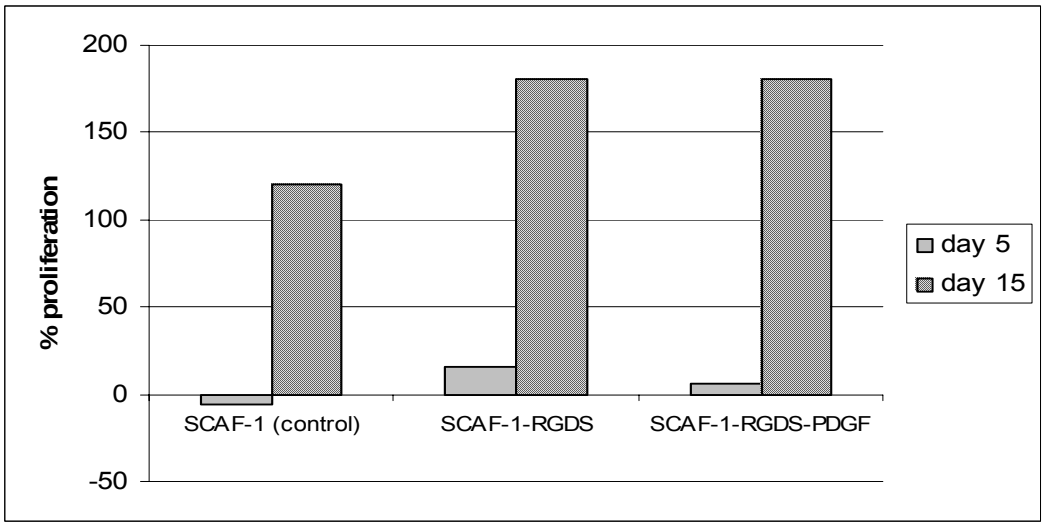

Figure 3.15 Percent proliferation of fibroblasts seeded on scaffolds in serum containing medium between day 5 and day 10, (OD at 492 nm), (n=6).

3.6.3 Florescence Microscopy

Primary human fibroblast cells were seeded on SCAF-1, SCAF-1-RGDS and SCAF-1-RGDS-PDGF and incubated for 15 days in serum free cell culture medium and examined under florescence microscopy on days 7 and 15 to observe cell viability, proliferation and distribution. Sections with 7μm thickness were taken with cryostat and cell nucleus staining was achieved with propidium iodide. Non-modified scaffold SCAF-1 served as control.

On day 7, control group scaffolds were lack of cell populated regions (Fig. 3.16 a) whereas highly proliferated cell regions were observed on RGDS and PDGF-BB modified scaffolds (Figure 3.16 b and c). These results support the MTT assay results so that, in serum free cell culture medium the scaffolds modified with RGDS and PDGF-BB provide better conditions for the attachment and proliferation of fibroblast cells.

On day 15 it could be seen that cell population has been increased on all groups of scaffolds (Figure 3.17). However modified scaffolds still preferred much more in serum free cell culture medium.

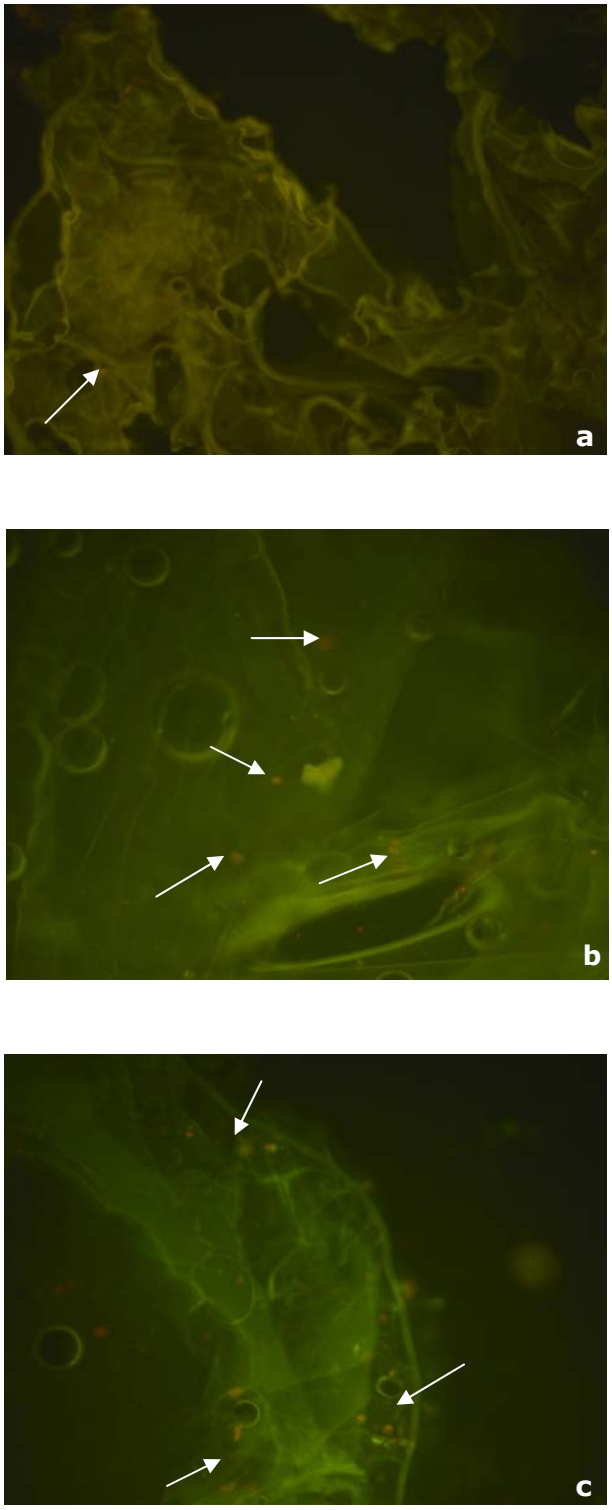

Figure 3.16 Florescence microscopy of fibroblast seeded scaffolds on day 7 incubated in serum free cell culture medium (a) SCAF-1 (control), (b) SCAF-1-RGDS, (c) SCAF-1-RGDS-PDGF (magnification 10X, arrows indicate cell regions).

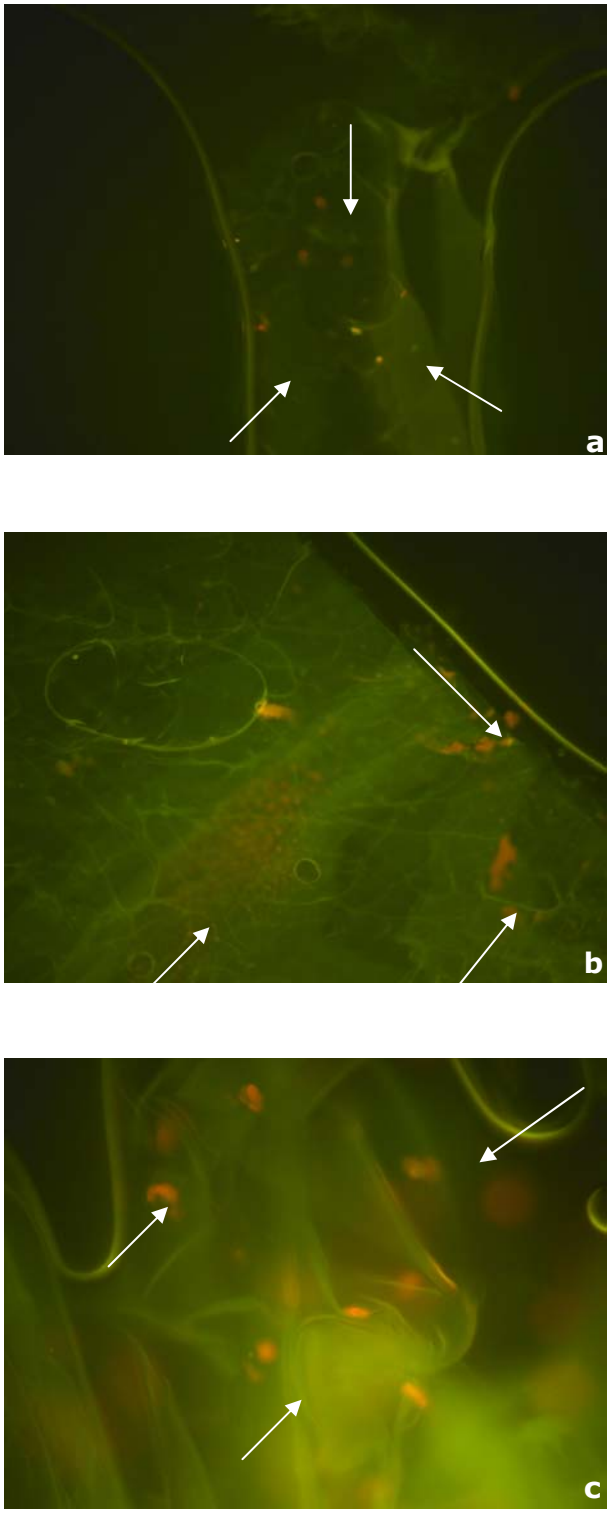

Figure 3.17 Florescence microscopy of fibroblast seeded scaffolds on day 15 incubated in serum free medium (a) SCAF-1 (control), (b) SCAF-1-RGDS, (c) SCAF-1-RGDS-PDGF (magnification 10X, arrows indicate cell regions).

3.6.4 Scanning Electron Microscopy Study

Attachment and morphology of fibroblasts that were seeded on scaffolds were studied with SEM after 2 hour, 7 day and 15 days of cultivation. Fibroblast cells attached on biomimetic scaffolds are clearly seen on Figure 3.18 and 3.19. In the natural environment fibroblast cells have spread and rod-like shapes [63]. The morphology of fibroblasts attached on scaffolds incubated both in serum and serum free media show differences with the incubation time periods (2 h, 7 days and 15 days). Fibroblasts have round, ball like shape at 2 h incubation (Figure 3.18a) and got spread shape on days 7 and 15 (Figure 3.18b). This indicate that cell at 2 h are not functionalized yet, whereas on day 7 they reach their native morphology. Another difference between initial and further stage of attachment is the bioactivity and proliferation of fibroblast cells. There are plaques around fibroblast cells attached on the scaffolds (Figure 3.18b and d) which are suggested to be the ECM that cells secreted on day 7 and day 15 samples. However at 2 h samples surroundings of cells are clear on any plaque formation (Figure 3.18a and c).

Cells seeded on scaffolds and incubated in serum free media did not show any differences in attachment and morphology when compared to ones incubated in serum containing media (Figure 3.19).

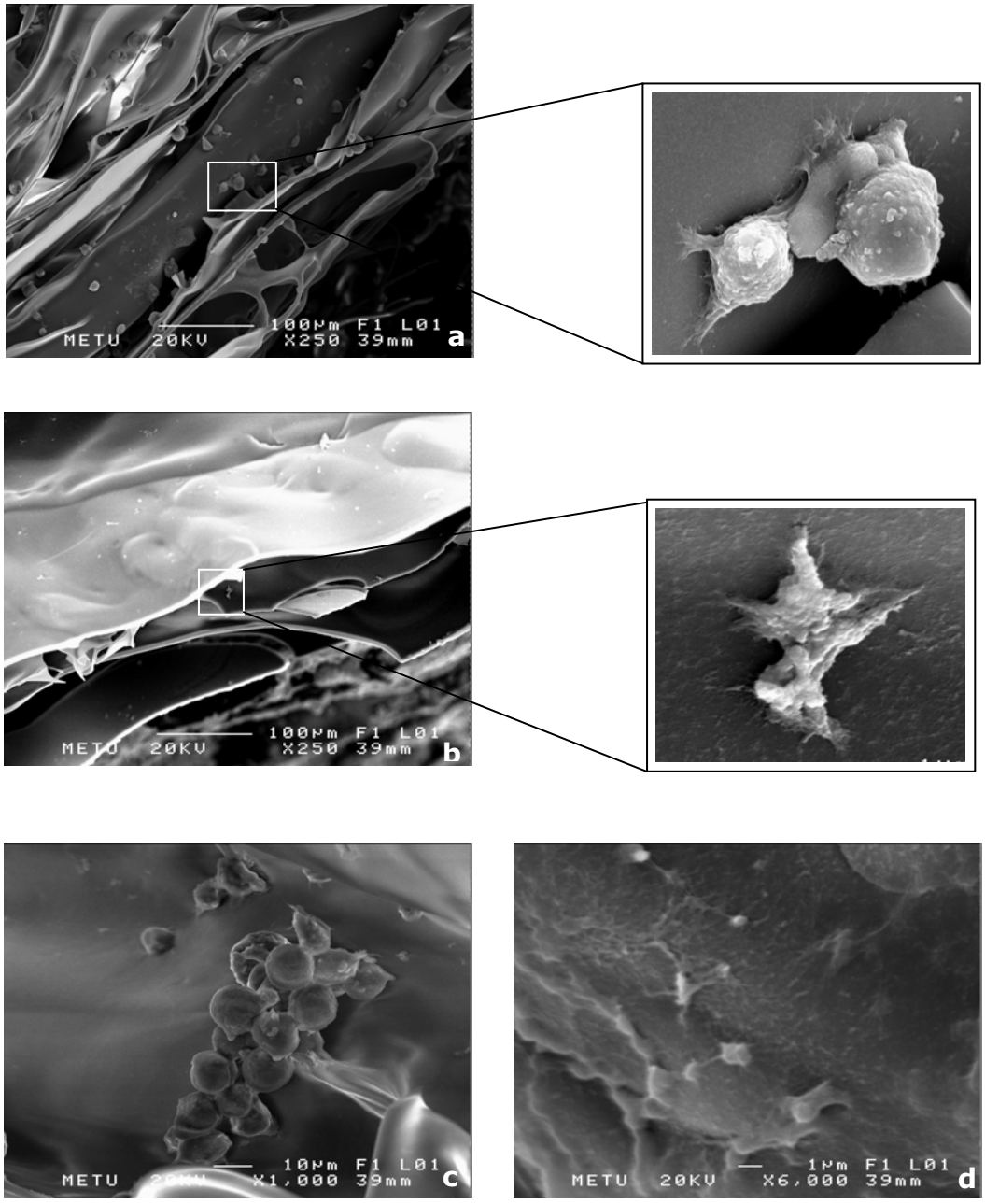

Figure 3.18 SEM images of fibroblast seeded scaffolds in serum free medium. (a) SCAF-1-RGDS at 2 h, (b) SCAF-1-RGDS on day 7, (c) SCAF-1-RGDS-PDGF at 2 h, (d) SCAF-1-RGDS-PDGF on day 7.

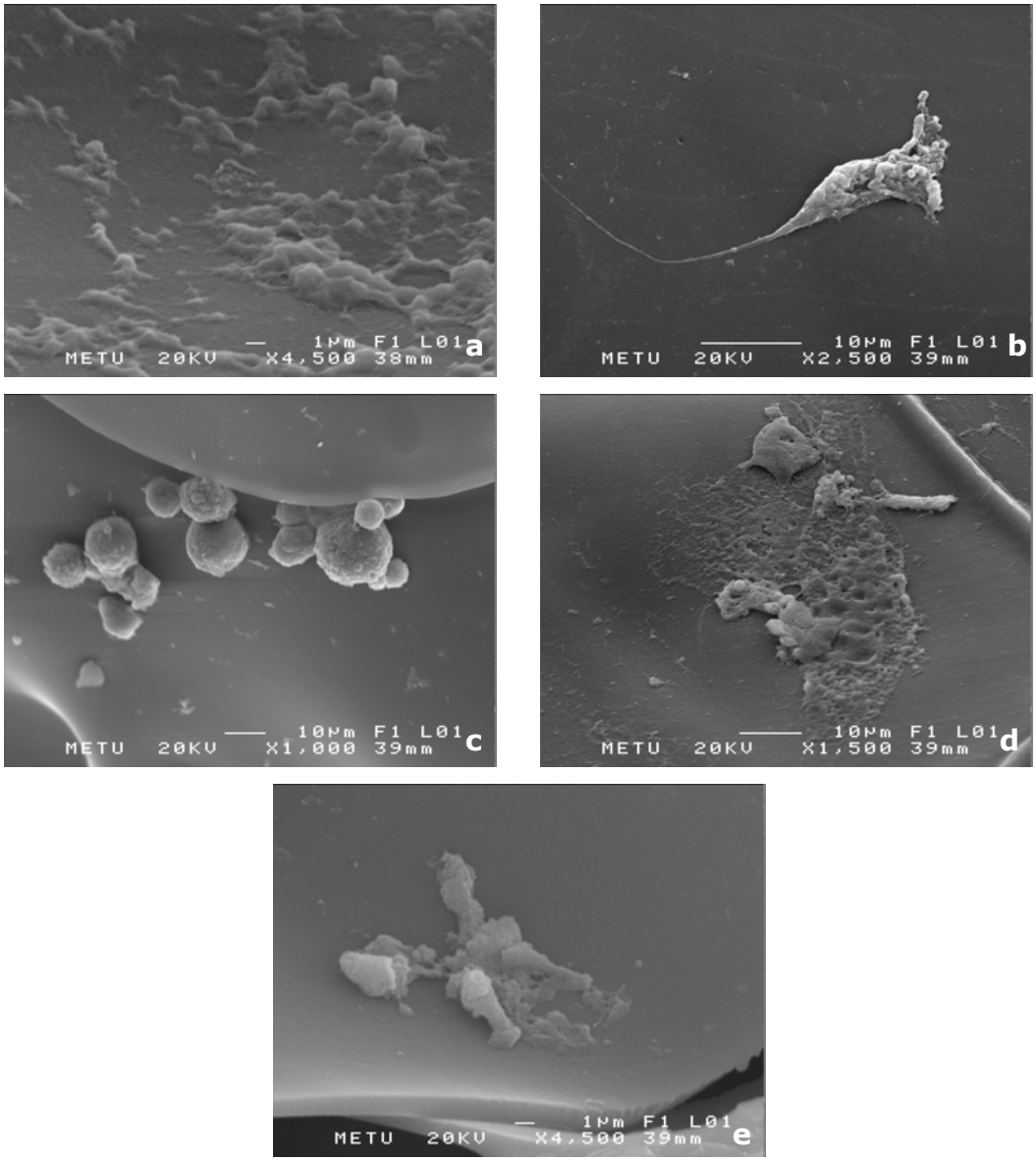

Figure 3.19 SEM images of fibroblast seeded scaffolds (a) SCAF-1 (control) in serum free at 2 h, (b) SCAF-1 (control) in serum containing medium on day 15, (c) cross-section of SCAF-1-RGDS-PDGF in serum free medium at 2h, (d) SCAF-1-RGDS-PDGF in serum containing medium on day 15, (e) SCAF-1-RGDS-PDGF in serum containing medium on day 7.

CHAPTER 4

CONCLUSION

Many synthetic or natural biomaterials have been developed as scaffolds for tissue engineering applications however there is not any structure totally mimicking extracellular matrix (ECM), ready to use yet.

In this study, integrated biomimetic scaffolds were developed by tissue engineering approach. Prepared scaffolds were composed of chitosan which can be considered as belonging to the family of glycosaminoglycan (GAG), gelatin and dermatan sulfate. Topography of scaffolds was designed by varying stirring rates and freezing temperatures. According to the results scaffolds prepared with 500 rpm stirring rate and frozen at -80 °C in cylindrical molds gave porous structure to provide sufficient space for cell growth and extracellular matrix production. Mechanical and enzymatic degradation results showed that scaffolds have physical integrity for use in tissue engineering applications. To stimulate and accelerate the cell adhesion and proliferation, biologically active peptide sequences of RGDS and growth factors were immobilized on optimized scaffolds. RGDS and RGDS-PDGF immobilized scaffolds demonstrated higher cell adhesion and proliferation compared to non-modified scaffolds even in serum free media. Morphology of fibroblasts attached on scaffolds reached native shape on day 7 and cells have begun secreting their ECM by that time. It can be concluded that RGDS-PDGF immobilized chitosan-gelatin-dermatan sulfate scaffolds could be considered as biomimetic scaffold candidates suitable to be used in soft tissue engineering applications.

REFERENCES

[1] Marler J. J., Upton J., Langer R., Vacanti J. P., "Transplantation of cells in matrices for tissue regeneration", Advanced Drug Delivery Reviews, 33: 65–182, 1998.

[2] Skalak R., Fox C. F., "Tissue engineering", Granlibakken, Lake Tahoe, Proceding workshop, New York, Liss, pp 26–29, 1988.

[3] Bloch J., Fine E. G., Bouche N., Anne D. Zurn A. D., Aebischer P., "Nerve Growth Factor- and Neurotrophin-3-Releasing Guidance Channels Promote Regeneration of the Transected Rat Dorsal Root", Experimental Neurology, 172: 425–432, 2001.

[4] Langer R., Vacanti J. P., "Tissue Engineering", Science, 260: 920-926, 1993.

[5] Fischbach C., "Adipose Tissue Engineering: Development of a 3-D Model System of Adipogenesis", Fakultät für Chemie und Pharmazie der Universität Regensburg, 2003.

[6] Gumbiner B. M., "Cell adhesion: the molecular basis of tissue architecture and morphogenesis", Cell, 84: 347–357, 1996.

[7] Garcia A., Collard D., Keselowsky B., Cutler S., Gallant N., Byers B., Stephanson S., "Engineering of Integrin-Specific Biomimetic Surfaces to Control Cell Adhesion and Function", in "Biomimetic Materials and Design", Edited by Dillow A. K., Lowman A. M., Marcel Dekker, New York, pp 30-53, 2002.

[8] Standard Guide for Characterization and Testing of Biomaterial Scaffolds Used in Tissue-Engineered Medical Products. American Society for Testing and Materials Standards, F2150-02e1, 2006.

[9] Murphy W. L., Mooney D. J., "Controlled delivery of inductive proteins, plasmid DNA and cells from tissue engineering matrices", J. Periodontal Res., 34: 413-419, 1999.

[10] Chaignaud B. E., Langer R., Vacanti J. P., in "Synthetic Biodegradable Polymer Scaffolds", Edited by Atala A., Mooney D. J., Birkhauser, Boston, MA, p. 1, 1997.

[11] Peppas N. A., Langer R. I., "New challenges in biomaterials", Science, 263: 715-1720, 1994.

[12] Mano J. F., Vaz C. M., Mendes S. C., "Dynamic mechanical properties of hydroxyapatite-reinforced and porous starch-based degradable biomaterials", J. Mater. Sci., 10: 857-862, 1999.

[13] Yang S., Leong K. F., Du Z., Chua C. K., "The design of scaffolds for use in tissue engineering. Part I. Traditional Factors", Tissue Engineering, 7: 679-689, 2001.

[14] Gilbert T. W., Sellaro T. L., Badylak S. F., "Decellularization of tissues and organs", Biomaterials, 27: 3675–3683, 2006.

[15] Mathew H. W. T., Polymers for Tissue Engineering Scaffolds, "In Polymeric Biomaterials", 2nd Rev. Edition Edited by Severian D., Marcel Dekker Incorporated, New York, p168, 2001.

[16] Lanza R. P., Langer R., Vacanti J., "Principles of Tissue Engineering", 2nd Edition, Academic Press, San Diego, p 264, 2000.

[17] Alberts B., Johnson A., Lewis J., Raff M., Roberts K., Walter P., "Molecular Biology of the Cell", 4th Edition, Garland Science Taylor and Francis Group, New York, p 96, 2002.

[18] Gelse K., Pöschl E., Aigner T., "Collagens—structure, function, and biosynthesis", Advanced Drug Delivery Reviews, 55: 1531–1546, 2003.

[19] Parry D., Steinert P., "Intermediate filaments: molecular architecture, assembly, dynamics and polymorphism", Quarterly Reviews of Biophysics, 32: 99–187, 1999.

[20] Muzzarelli R. A. A., "Biochemical significance of exogenous chitins and chitosans in animals and patients", Carbohydrate Polymers, 20: 7–16, 1993.

[21] Kuijpers A. J., Engbers G. H., Krijgsveld J., Zaat S. A., Dankert J., Feijen J., "Cross-linking and characterisation of gelatin matrices for biomedical applications", J. Biomater. Sci., Polym. Ed., 11: 225–243, 2000.

[22] Mao J., Zhao L., Yao K., Shang Q., Yang G., Cao Y., "Study of novel chitosan-gelatin artificial skin *in vitro*", J. Biomed Mater Res, 64A: 301–308, 2003.

[23] Ikada Y., Tabata Y., "Protein release from gelatin matrices", Adv. Drug Delivery Rev., 31: 287–301, 1998.

[24] Young S., Wong M., Tabata Y., Mikos A. G., "Gelatin as a delivery vehicle for the controlled release of bioactive molecules", Journal of Controlled Release 109: 256–274, 2005.

[25] Hirano S., Tsuchida H., Nagao N., "N-Acetylation in chitosan and the rate of its enzymic hydrolysis", Biomaterials, 10: 574-576, 1989.

[26] Chupa I. M., Foster A. M., Sumner S. R., Madihally S. V., Mathew H. W., "Vascular cell responses to polysaccharide materials: in vitro and in vivo evaluations", Biomaterials 21: 2315-2322, 2000.

[27] Elcin A. E., Elcin Y. M., Peppas G. D., "Neutral tissue engineering: adrenil chromaffin cell attachment and viability on chitosan scaffolds", Neurol Res, 20: 648-654, 1998.

[28] Elcin Y. M., Dixit V., Lewin K., Gitnick G., "Xenotransplantation of fetal porcine hepatocites in rats using a tissue engineering approach", Artif Organs, 23: 146-152, 1999.

[29] Madihally S. V., Matthew H. W. T., "Porous chitosan scaffolds for tissue engineering", Biomaterials, 20: 1133-1142, 1999.

[30] Mathew H. W. T., "Chitosan as a Molecular Scaffold for Biomimetic Design of Glycopolymer Biomaterials", in Biomimetic Materials and Design: Biointerfacial Strategies, Tissue Engineering, and Targeted Drug Delivery, Edited by Dillow A., Lowman A., Marcel Dekker Incorporated, New York, pp 311- 320, 2002.

[31] Ma P. X., "Scaffolds for tissue fabrication", Materials Today, 30-40, May 2004.

[32] Ma P. X., "Tissue Engineering", in Encyclopedia of Polymer Science and Technology, 3rd Edition, Edited by Kroschwitz, J. I., John Wiley & Sons, NJ, 2004.

[33] Ma P. X., Langer R., "Degradation, structure and properties of fibrous poly(glycolic acid) scaffolds for tissue engineering" in Polymers in Medicine and Pharmacy, Edited by Mikos, A. G., et al., Materials Research Society, p 99, 1995.

[34] Zhang R., Ma P. X., "Degradation behavior of porous poly(a-hydroxy acids)/hydroxyapatite composite scaffolds", ACS Polymer Preprint, 41: 1618-1619, 2000.

[35] Pitt C. G., "Poly-ε-caprolactone and its copolymers", in Biodegradable Polymers as Drug Delivery Systems, Edited by Chasin M., Langer R., Dekker, New York, pp 71-119, 1990.

[35] Mathew H. W. T., "Polymers for Tissue Engineering Scaffolds", In Polymeric Biomaterials, 2nd Rev. Edition Edited by Severian D., Marcel Dekker Incorporated, New York, pp180-181, 2001.

[37] Landeen L. K., Zeigler F. C., Halberstadt C., "Characterization of a human dermal replacement", Wounds, 5: 167-175, 1992.

[38] Mikos A. G., Bao Y., Linda L. G., "Preparation of poly(glycolic acid) bonded fiber structures for cell attachment and transplantation", J. Biomed. Mater. Res., 27: 183-189, 1993.

[39] Nam Y. S., Park T. G., "Biodegradable polymeric microcellular foams by modified thermally induced phase separation method", Biomaterials, 20: 1783-1790, 1999.

[40] Mikos A. G., Sarakinos G., Vacanti J. P., "Biocompatible polymer membranes and methods of preparation of three dimensional membrane structures", U.S. patent 5, 514, 378.

[41] Yang S., Leong K. F., Du Z., Chua C. K., "The Design of scaffolds for use in tissue engineering Part II. Rapid Prototyping Techniques", Tissue Engineering, 8: 1-11, 2002.

[42] Ruoslahti E., Pierschbacher M. D., "New perspectives in cell adhesion: RGD and integrins", Science, 238: 491–7, 1987.

[43] Pierschbacher M. D., Ruoslahti E., "Cell attachment activity of fibronectin can be duplicated by small synthetic fragments of the molecule", Nature, 309: 30–33, 1984.

[44] Hersel U., Dahmen C., Kessler H., "RGD modified polymers: biomaterials for stimulated cell adhesion and beyond", Biomaterials, 24: 4385–4415, 2003.

[45] Bowen-Pope D. F., Malpass T. W., Foster D. M., Ross R., "Platelet-derived growth factor in vivo: Levels, activity, and rate of clearance", Blood, 64: 458–469, 1984.

[46] Babensee J. E., McIntire L. V., Mikos A. G., "Growth factor delivery for tissue engineering", Pharmaceutical Research, 17: 497-504, 2000.

[47] Wei G., Jin Q., Giannobile W. V., Ma P. X., "Nano-fibrous scaffold for controlled delivery of recombinant human PDGF-BB", Journal of Controlled Release, 112: 103–110, 2006.

[48] Robson M. C., Mustoe T. A., Hunt T. K., "The future of recombinant growth factors in wound healing", Am. J. Surg. 176:2A, 80–82, 1998.

[49] Becker W. M., Kleinsmith L. J., Hadin J., "The world of the cell" 6th edition, Pearson Benjamin Cummings, San Francisco, pp 484-485, 2006.

[50] Saltzman W. M., "Tissue Engineering Principles for the Design of Replacement of Organs and Tissues", Oxford University Press, pp 173 – 178, 2004.

[51] Hoa M. H., Wanga D. M., Hsieha H. J., Liub H. C., Hsienc T. Y., Laid J. Y., Hou L. T., "Preparation and characterization of RGD-immobilized chitosan scaffolds", Biomaterials, 26: 3197–3206, 2005.

[52] Zhang L., Ao Q., Wang A., Lu G., Kong L., Gong Y., Zhao N., Zhang X., "A sandwich tubular scaffold derived from chitosan for blood vessel tissue engineering", J Biomed Mater Res, 77A: 277–284, 2006.

[53] Huang Y., Siewe M., Madihally S. V., "Effect of Spatial Architecture on Cellular Colonization", Biotechnology and Bioengineering, 93: 64-75, 2006.

[54] Dillaman R., Hequembourg S., Gay M., "Early Pattern of Calcification in the Dorsal Carapace of the Blue Crab, *Callinectes sapidus*", Journal of Morphology, 263: 356–374, 2005.

[55] Eiselt P., Yeh J., Latvala R. K., Shea L. D., Mooney D. J., "Porous carriers for biomedical applications based on alginate hydrogels", Biomaterials, 21: 1921-1927, 2000.

[56] Starlya B., Laub W., Bradburyb T., Sun W., "Internal architecture design and freeform fabrication of tissue replacement structures", Computer-Aided Design, 38: 115–124, 2006.

[57] Karageorgiou V., Kapan D.,"Porosity of 3D biomaterial scaffolds and osteogenesis", Biomaterials, 26: 5474-5491, 2005.

[58] Buttafoco L., Buijtenhuijs P., Poot A., Dijkstra P., Daamen W., Kuppevelt T., Vermes I., Feijen J., "First Steps Towards Tissue Engineering of Small-Diameter Blood Vessels: Preparation of Flat Scaffolds of Collagen and Elastin by Means of Freeze Drying", J. Biomed Mater Res Part B: Appl Biomater, 77B: 357–368, 2006.

[59] Domard A.,Domard M., "Chitosan: Structure – Properties Relationship and Biomedical Applications", in Polymeric Biomaterials, 2nd Rev. Edition Edited by Severian D., Marcel Dekker Incorporated, New York, pp187-212, 2001.

[60] Yannas V., Burke J. F., Design of an artificial skin, 1. Basic design principles, J Biomed Mater Res., 14: 65–81, 1980.

[61] Drumheller P. D., Hubbell J. A., "Surface Immobilization of Adhesion Ligands for Investigations of Cell-Substrate Interactions" in The Biomedical Engineering Handbook, 2nd Edition, Edited by Bronzino D. J., CRC Press LLC, Boca Raton, chapter 110, 2000.

[62] Lv Q., Feng Q., Hu K., Cui F., "Three-dimensional fibroin/collagen scaffolds derived from aqueous solution and the use for HepG2 culture", Polymer, 46: 12662-12669, 2005.

[63] Hou T., Zhang J. Z., Kong L. J., Zhang X. F., Hu P., Zhang D. M., Li N., "Morphologies of fibroblast cells cultured on surfaces of PHB films implanted by hydroxyl ions", J. Biomater Sci Polymer Edn, 17:7, 735–746, 2006.

APPENDICES

APPENDIX A

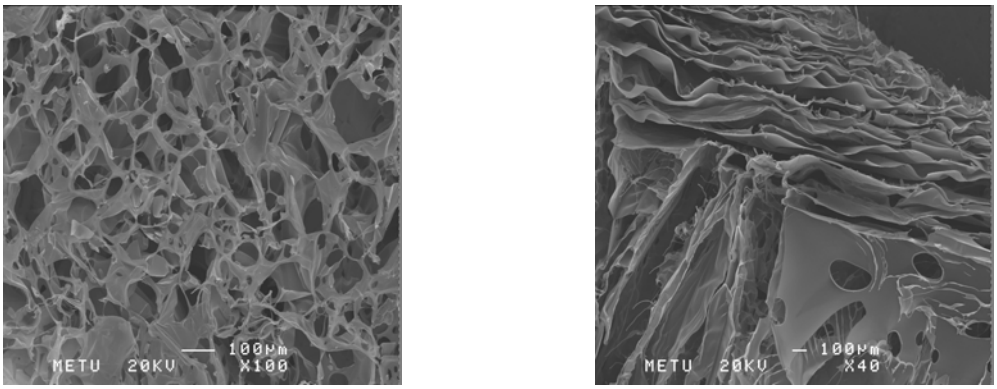

Figure A.1 SEM image of chitosan (1 % w/v) stirred at 2000 rpm.

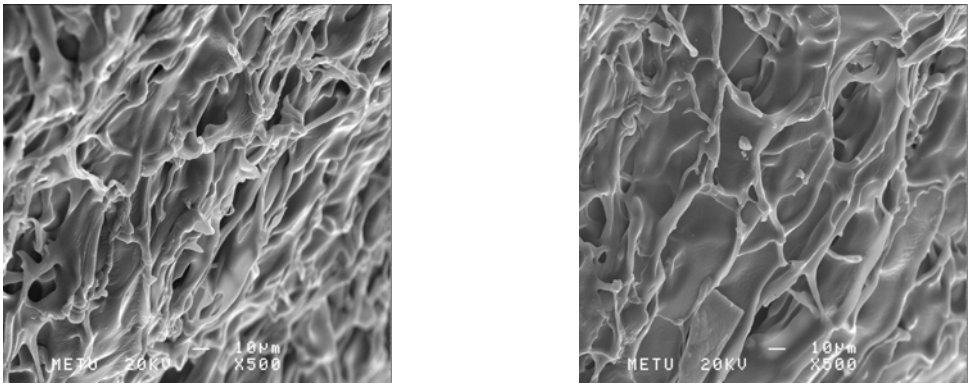

Figure A.2 SEM image of Chitosan-Gelatin (1 % w/v with 2.6:1 ratio) + Glycerol (2 % v/v) stirred at 2000 rpm.

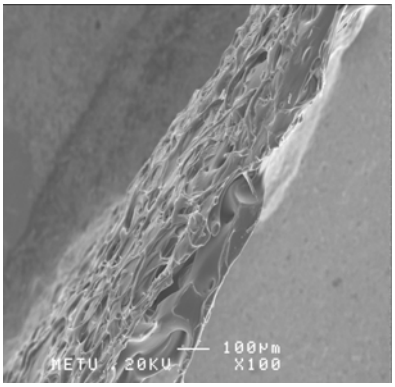

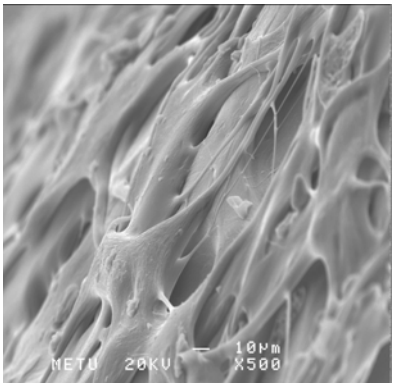

Figure A.3 SEM image of Chitosan-Gelatin (1 % w/v with 2.6:1 ratio) + Glycerol (1 % v/v) stirred at 2000 rpm.

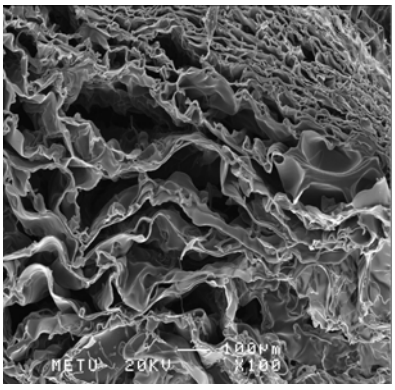

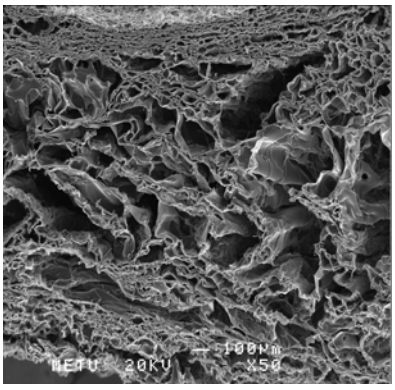

Figure A.4 SEM image of Chitosan-Gelatin (1 % w/v with 4:1 ratio) + Glycerol (1 % v/v) stirred at 2000 rpm.

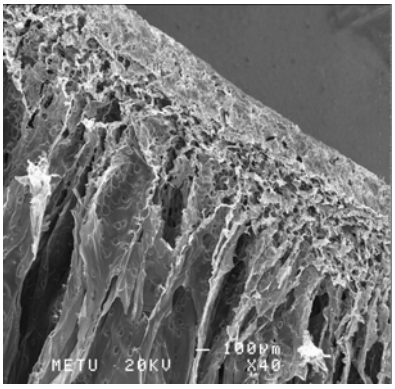

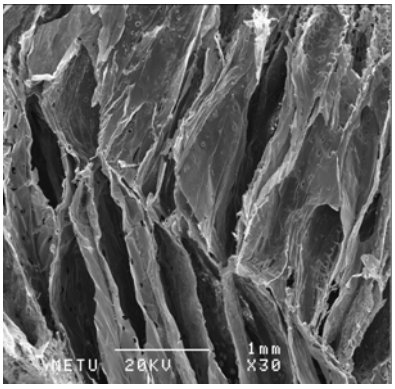

Figure A.5 SEM image of Chitosan-Gelatin (1 % w/v with 4:1 ratio) + Dermatan Sulfate (0.03 % w/w) stirred at 2000 rpm.

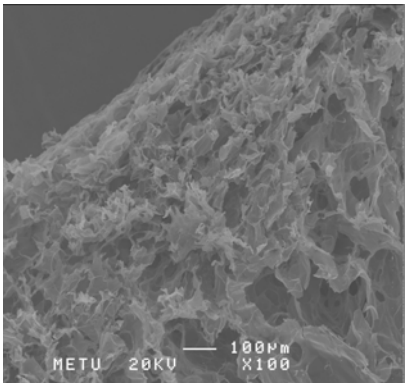

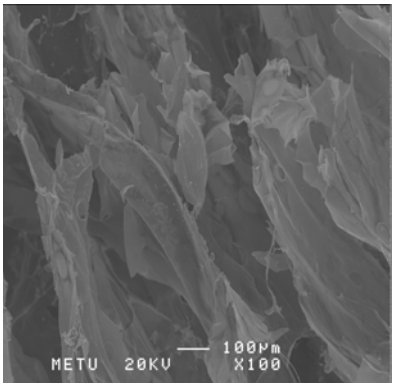

Figure A.6 SEM image of Chitosan-Gelatin (1 % w/v with 4:1 ratio) + Dermatan Sulfate (0.03 % w/w) stirred at 2000 rpm and crosslinked with glutaraldehyde.

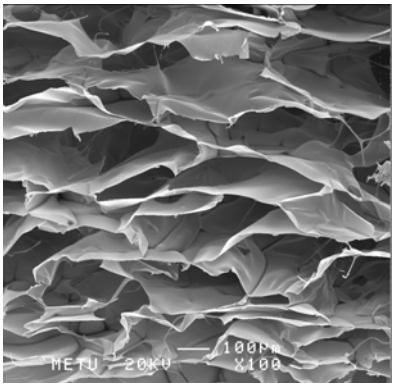

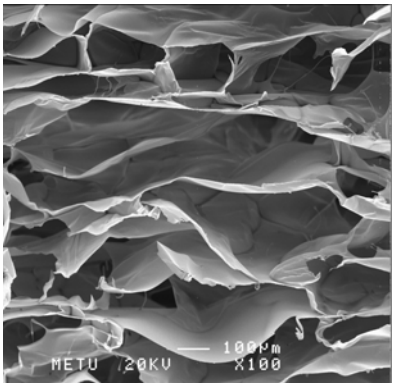

Figure A.7 SEM image of Chitosan-Gelatin (1 % w/v with 1:1 ratio) + Dermatan Sulfate (0.03 % w/w) stirred at 500 rpm.

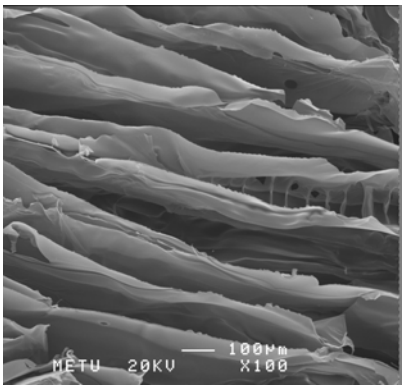

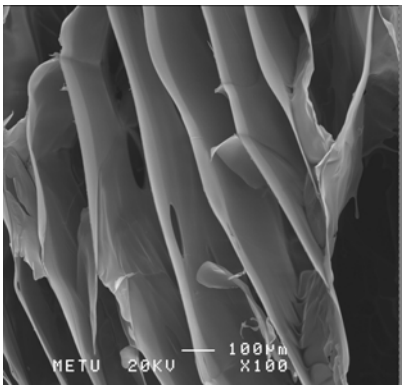

Figure A.8 SEM image of Chitosan-Gelatin (1.5 % w/v with 4:1 ratio) + Dermatan Sulfate (0.03 % w/w) stirred at 500 rpm.

APPENDIX B

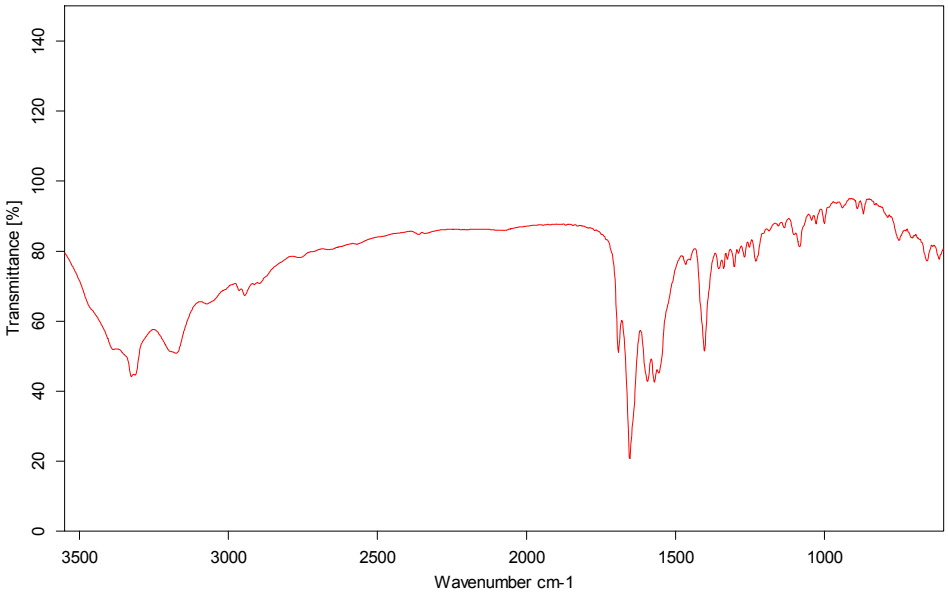

Figure B.1 FTIR spectra of RGDS peptide in KBr.

APPENDIX C

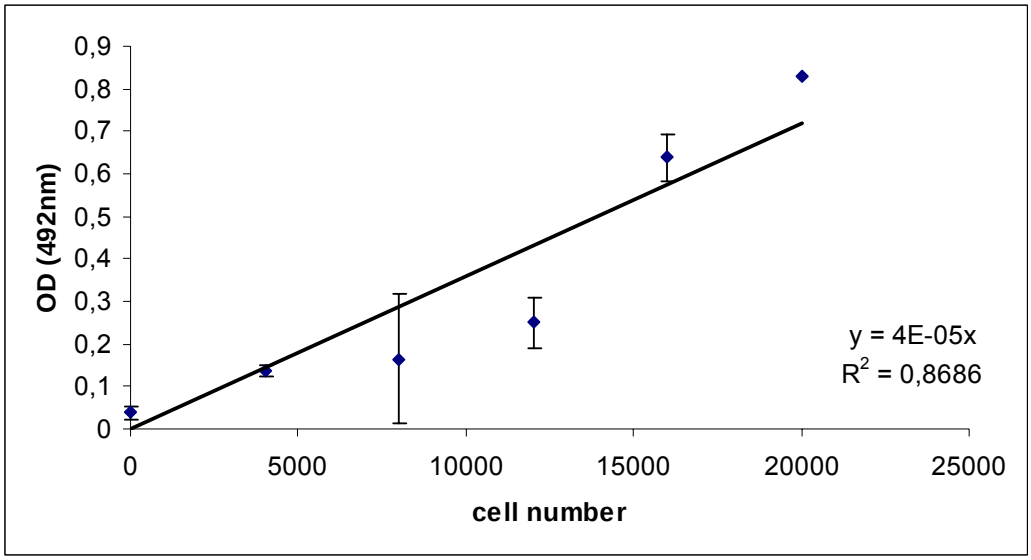

Figure C.1 Calibration curve for fibroblast cells obtained by MTT assay.